

Klaus Grieshofer

Estimation of Reaction Rates from Fluorescence Recovery after Photobleaching

Diploma Thesis



Institute of Medical Engineering
Graz University of Technology
Kronesgasse 5, A - 8010 Graz
Head: Univ.-Prof.Dipl.-Ing.Dr.techn. Rudolf Stollberger

Supervisor: Univ.-Prof.Dipl.-Ing.Dr.techn. Paul Wach

Evaluator: Univ.-Prof.Dipl.-Ing.Dr.techn. Paul Wach

Graz, 2012/01

Abstract

Fluorescence recovery after photobleaching [FRAP] is a fluorometric measurement technique that holds information on the mobility of fluorescently labeled molecules. In the nucleus of a living cell the mobility is mainly depending on restricted diffusion and binding site interaction. The reaction rates of the binding site interaction can be estimated by a suitable model of FRAP. Therefore this work contains the development of a model and the parameter identification. The model is described by a Bessel series expansion and it is extended to a disk model and a ring model to gain better estimations by spatial information. The parameter identification is performed with the weighted least square estimator with Gauss-Newton iteration step update. To cover a wide range of possible FRAP experiments with different reaction rates, the chosen regularization is a truncated singular values decomposition with an adapting truncation parameter. Also Matlab's solver tools are implemented for parameter identification and the estimators are investigated with respect to different advantages. It is shown that the estimation of the reaction rates can be performed with moderate computational effort.

Zusammenfassung

Fluorescence recovery after photobleaching [FRAP] ist ein fluorometrisches Messverfahren bei dem man Informationen über die Beweglichkeit von fluoreszent markierten Molekülen erhält. Im Nukleus einer lebenden Zelle ist die Beweglichkeit der Moleküle hauptsächlich von Diffusion und Wechselwirkungen mit Bindungsstellen abhängig. Mit einem geeigneten Modell kann die Reaktionsgeschwindigkeit der Wechselwirkung mit Bindungsstellen bestimmt werden. Diese Arbeit leitet ein Modell und die Parameteridentifikation für die Reaktionsgeschwindigkeiten her. Das Modell basiert auf einer Besselreihenentwicklung und wird zu einem Scheibenmodell und einem Ringmodell weiterentwickelt, um die Parameterbestimmung durch zusätzliche Ortsinformation zu verbessern. Die Parameterbestimmung wird mittels Weighted-Least-Square-Schätzer mit Gauß-Newton Iterationsschritt-Aktualisierung realisiert. Um viele mögliche FRAP Experimente mit unterschiedlichen Reaktionsgeschwindigkeiten bearbeiten zu können wurde die Truncated Singular Value Decomposition mit adaptiven Truncationparameter als Regularisierung gewählt. Die Parameteridentifikation ist auch mittels Matlabs solver Funktionen umgesetzt und die Schätzer wurden auf ihre Vorteile hin untersucht. Wie hier gezeigt, ist die Parameteridentifikation mit angemessenem Rechenaufwand umsetzbar.

STATUTORY DECLARATION

I declare that I have authored this thesis independently, that I have not used other than the declared sources / resources, and that I have explicitly marked all material which has been quoted either literally or by content from the used sources.

.....

date

.....

signature

Contents

List of Symbols	1
1 Introduction	3
1.1 Fluorescence Recovery After Photobleaching	3
1.2 Objectives	4
2 Methods	5
2.1 Solution of the Partial Differential Equations	5
2.2 Series Expansion for the Sums of the Unbleached Concentrations $frap(r, t)$	9
2.3 Approximating the Initial Distribution by Linear and Quadratic Terms . .	10
2.4 Set of Analytical Formulas for the Forward Problem	16
2.5 Parameter Estimation	16
2.6 Set of Analytical Formulas for the Inverse Problem	17
2.7 Numerical Representation of $Frap(t)$	21
2.8 Set of Numerical Formulae for the Inverse Problem	22
2.9 Implementation of the Estimation	25
2.9.1 Covariance Matrix	28
2.10 Spatial FRAP Model	28
3 Results	32
3.1 Determining K_b	32
3.2 Estimation of K_1 and K_2	33
3.2.1 Effect of the Number of Terms of Bessel Series	34
Effect on Approximating the Initials Distribution	34
Effect on Estimation	34
3.2.2 Sensitivity to the Choice of Start Parameters	36
3.2.3 Comparison of Estimators	40
3.2.4 Covariance of Weighted Least Square Estimator	41
3.3 Estimation of K_1 , K_2 and D	41
3.3.1 Effect of the Number of Terms of Bessel Series	41
Effect on Estimation	41
3.3.2 Sensitivity to the Choice of Start Parameters	43
Estimation of K_1 , K_2 and D	44
Estimation of K_1 , K_2 and D by Disk-Model	46
Estimation of K_1 , K_2 and D by Ring-Model	49
3.3.3 Comparison of Estimators	53
4 Conclusion	54
4.1 Number of Terms for the Bessel Series expansion	54
4.2 Estimation of K_1 and K_2	54
4.2.1 Ring and Disk Estimation	55
Comparison of the Results	55
Covariance Matrix	56
Sensitivity to Choice of Start Parameter	56
4.3 Estimation of K_1 , K_2 and D	56
Comparison of the Results	57

Estimation of D	57
References	58
A Appendix	60
A.1 Determination of Integral over Bessel Functions with Orthogonality Relations	60
A.2 Detailed Solution Method for Calculating the Coefficients of the Bessel Series	61
A.3 Coefficients' Dependence on K_b	64
A.4 Detailed Partial Derivatives for Frap, Jacobian and rearranged Hessian . .	64
A.5 Differentiation with the Symbolic Toolbox	67

List of Symbols

Symbol	Unit	Description
a	$[m^{-1}]$	variable for approximation of $h(r, 0)$
A_k	[1]	coefficient for Bessel series expansion of solution for $f1$
a_k	[1]	coefficient for Bessel series expansion of solution of $c1$
α_k	[1]	to wR scaled zeros of first kind and first order Bessel function
b	$[m^{-1}]$	variable for approximation of $h(r, 0)$
β_k	$[s^{-1}]$	exponential coefficient of Bessel series expansion of solution for $f1$ and $c1$
B_k	[1]	coefficient for Bessel series expansion of solution for $f1$
b_k	[1]	coefficient for Bessel series expansion of solution of $c1$
C_{eq}	[1]	state of equilibrium for bound molecules
C	[1]	concentration of bound fluorescence molecules
$c1_k$	[1]	particular solution for system of differential equation
$c1$	[1]	substitution for unbleached molecules
c	[1]	concentration of bound fluorescence molecules
χ_k	[1]	zeros of first kind and first order Bessel function
D	$[\frac{m^2}{s}]$	constant of diffusion
E_k	[1]	coefficients of Bessel series expansion for approximation of $h(r, 0)$
F_{eq}	[1]	state of equilibrium for free molecules
F	[1]	concentration of free fluorescence molecules
$f1_k$	[1]	particular solution for system of differential equation
$f1$	[1]	substitution for unbleached molecules
f	[1]	concentration of free fluorescence molecules
frap	[1]	sum of concentration of unbleached molecules
$frap(r, t)$	[1]	sum of the concentrations of unbleached molecules
γ_k	$[s^{-1}]$	exponential coefficient of Bessel series expansion of solution for $f1$ and $c1$
$h1$	[1]	substitution for unbleached molecules
h	[1]	sum of concentration of bleached molecules
$h(r, 0)$	[1]	initial distribution of sum of concentrations of bleached molecules
I_1	[1]	auxiliary variable for determination of E_k
I_2	[1]	auxiliary variable for determination of E_k
I_3	[1]	auxiliary variable for determination of E_k
J_0	[1]	Bessel function of first kind and zeroth order
J_1	[1]	Bessel function of first kind and first order
K_1	$[s^{-1}]$	on rate for fluorescence molecules at the presence of binding sites
k	[1]	index of Bessel series expansion
K_2	$[s^{-1}]$	off rate for fluorescence molecules at the presence of binding sites

Symbol	Unit	Description
K_b	$[s^{-1}]$	rate constant of bleaching due to imaging
R	$[m]$	spot radius of ROI
r	$[m]$	radius
S	$[1]$	concentration of binding sites for fluorescence molecules
σ	$[m]$	inflection point of the gaussian decay
t	$[s]$	time
θ	$[1]$	residual fluorescence level after bleaching
u	$[1]$	auxiliary variable for substitution
v_k	$[s^{-1}]$	auxiliary variable for determination of coefficients for Bessel expansion for the solution of $c1$ and $f1$
w_k	$[s^{-1}]$	auxiliary variable for determination of coefficients for Bessel expansion for the solution of $c1$ and $f1$
X	$[m]$	auxiliary variable for determination of E_k
x_b	$[m]$	variable for approximation of $h(r, 0)$
x_c	$[m]$	variable for approximation of $h(r, 0)$
x_d	$[m]$	variable for approximation of $h(r, 0)$
x_p	$[m]$	variable for approximation of $h(r, 0)$
$y_G(r)$	$[1]$	function of gaussian decay
$y_{lP}(r)$	$[1]$	lower parabola for approximation of $h(r, 0)$
$y_T(r)$	$[1]$	linear function in inflection point σ
$y_{uP}(r)$	$[1]$	upper parabola for approximation of $h(r, 0)$
z	$[1]$	auxiliary variable for determination of E_k

1 Introduction

1.1 Fluorescence Recovery After Photobleaching

Fluorescence recovery after photobleaching [FRAP] is a fluorometric measurement technique of optical microscopy. Fluorescent molecules in the a region of interest [ROI] are irreversibly bleached by a laser. The measurement of the recovery of the fluorescence in the ROI is monitored by the same laser. The recovery represents the mobility of the fluorescent molecules from surrounding area. The recovery is determined by the diffusion of the fluorescent molecules and, in the presence of binding sites for the fluorescent molecules, the reaction rate constants. The observation light bleaches a small amount of the fluorescent molecules during the measurement, this effect is called bleaching due to imaging. The recovery data can be analyzed to determine those parameters when there is an suitable FRAP model at hand.[8, 1, 9] Therefore the FRAP model is mainly important for the accuracy of the parameter identification. For data analysis the raw FRAP data are

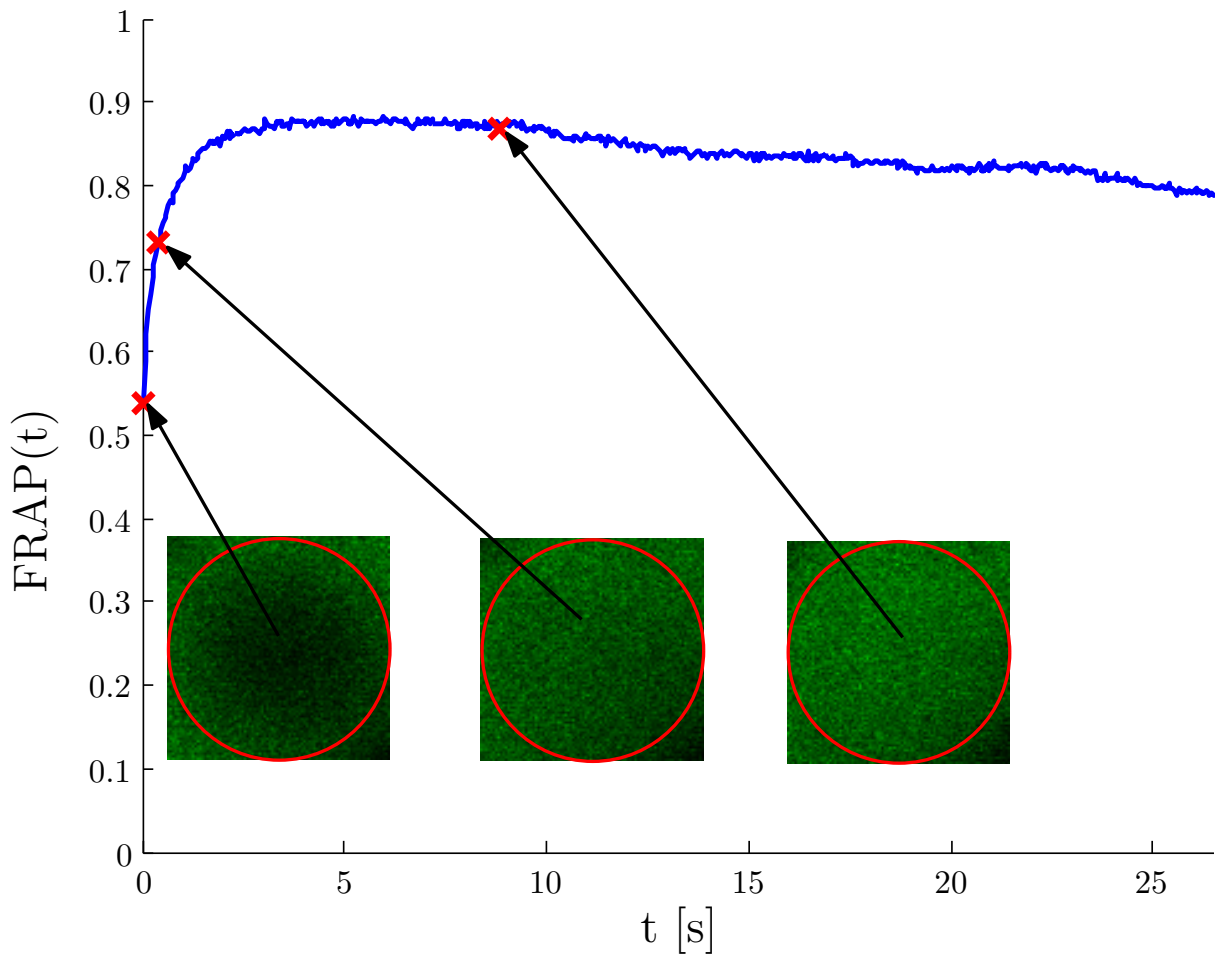


Figure 1: FRAP-curve with corresponding raw data

depicted as intensities, that have been averaged over the ROI and are normalized. This

is illustrated by figure 1. The considered FRAP measurements are performed in living cells. This work describes a FRAP model that reproduces the processes of:

- restricted diffusion
- bleaching due to imaging
- single binding interaction

The attributes of this FRAP model are:

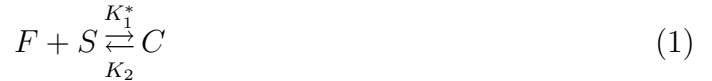
- cylindric symmetry
- gaussian decay for the bleaching border
- bleaching due to imaging has a constant rate
- reaction rates are constant
- diffusion is constant over time and space
- homogeneous volume
- known ratio of radius of bleaching spot to radius of cell nucleus

1.2 Objectives

This work shows the mathematical formulation of the introduced FRAP model and its numerical implementation. For the subsequent data analysis of FRAP experiments different approaches for parameter identification are established. The FRAP model is extended to a spatial FRAP model to improve the parameter identification. The ability of the parameter identification is investigated with respect to the predictability of different parameters.

2 Methods

FRAP is a measurement technique of the optical microscopy. Fluorescently marked molecules are observed in a cell, bleached by a laser and the subsequent recovery is measured. At the presence of single binding sites for those molecules the reaction kinetics is described by equation (1). F is the concentration of the free molecules, C the concentration of the bound molecules and S is the concentration of binding sites for the molecules. The considered concentrations are bleached concentration.



K_1^* and K_2 are the on and off rates for the binding reactions. Through the bleaching process the concentration S is constant and so the partial differential system for the concentrations is presented [9].

$$F_{eq} = \frac{K_2}{K_1 + K_2} \quad (2a) \quad C_{eq} = \frac{K_1}{K_1 + K_2} \quad (2b)$$

$$\frac{\partial f}{\partial t} = D \Delta f - K_1 f + K_2 c \quad (3a)$$

$$\frac{\partial c}{\partial t} = K_1 f - K_2 c \quad (3b)$$

This partial differential system is solved through a Bessel series expansion. The partial differential system describes the concentrations of bound bleached molecules c and free bleached molecules f . F_{eq} and C_{eq} are the equilibrium states of the reaction, D is the diffusion constant.

2.1 Solution of the Partial Differential Equations

Considering bleaching due to imaging with a rate K_b the partial differential equation system for the concentrations of bleached particles, can be written

$$\frac{\partial f}{\partial t} = D \Delta f - (K_1 + K_b) f + K_2 c + F_{eq} K_b \quad (4a)$$

$$\frac{\partial c}{\partial t} = K_1 f - (K_2 + K_b) c + C_{eq} K_b \quad (4b)$$

The state of equilibrium for the concentrations is

$$F_{eq} = \frac{K_2}{K_1 + K_2} \quad (5a)$$

$$C_{eq} = \frac{K_1}{K_1 + K_2} \quad (5b)$$

$$h = f + c \quad \dots \quad \text{sum of the concentrations of bleached particles} \quad (6a)$$

$$\text{frap} = (1 - h) \quad \dots \quad \text{sum of the concentration of unbleached particles} \quad (6b)$$

Substituting the negative concentration of unbleached particles for c and f the partial differential equation system can be rewritten

$$f1 = f - F_{eq} \quad (7a) \quad c1 = c - C_{eq} \quad (7b)$$

$$K_1 F_{eq} = K_2 C_{eq} \quad (8)$$

$\frac{\partial f1}{\partial t} = D \Delta f1 - (K_1 + K_b) f1 + K_2 c1 \quad (9a)$	(9a)
$\frac{\partial c1}{\partial t} = K_1 f1 - (K_2 + K_b) c1 \quad (9b)$	(9b)

$$h1 = f1 + c1 = c + f - 1 = -(1 - h) \quad (10a)$$

$$h = h1 + 1$$

$$\text{frap} = -h1 = (1 - h) \quad \dots \quad \text{sum of the concentration of all unbleached particles} \quad (10b)$$

Particular solutions for equations (9a) and (9b) are:

$f1_k = \left(A_k e^{-\beta_k t} + B_k e^{-\gamma_k t} \right) J_0(\alpha_k r) \quad (11a)$	(11a)
$c1_k = \left(a_k e^{-\beta_k t} + b_k e^{-\gamma_k t} \right) J_0(\alpha_k r) \quad (11b)$	(11b)

Considering restricted diffusion for boundary $r = wR$ ($w > 1$), where R is the spot radius of the ROI, leads to

$$\alpha_k wR = \chi_k \quad \alpha_k = \frac{\chi_k}{wR} \quad \alpha_0 = 0 \quad (12)$$

Where χ_k is the k -th zero of the Bessel function of the first kind and first order. By this definition the diffusion fluxes are forced to be zero at $r = wR$, because the spatial derivative of $J_0(\alpha_k r)$ can be expressed in terms of $J_1(\alpha_k r)$. Inserting the equations (11a)

and (11b) and the following identity:

$$\frac{\partial^2}{\partial r^2} J_0(\alpha_k r) + \frac{1}{r} \frac{\partial}{\partial r} J_0(\alpha_k r) + \alpha_k^2 J_0(\alpha_k r) \equiv 0$$

into (9a) and (9b) and equating the coefficients of $e^{-\beta_k t}$ and $e^{-\gamma_k t}$ the following equations are obtained.

$$a_k = A_k \frac{-\beta_k + D\alpha_k^2 + K_1 + K_b}{K_2} \quad (13a)$$

$$= A_k \frac{K_1}{-\beta_k + K_2 + K_b} \quad (13b)$$

$$b_k = B_k \frac{-\gamma_k + D\alpha_k^2 + K_1 + K_b}{K_2} \quad (14a)$$

$$= B_k \frac{K_1}{-\gamma_k + K_2 + K_b} \quad (14b)$$

From (13a), (13b) and (14a), (14b) follows an equation for β_k and γ_k , because the equations (13a), (13b) must hold at the same time, as well as (14a), (14b). The two equations are quadratic and have identical solutions. Therefore only one equation is solved and the first solution is assigned to β_k the second one to γ_k . With

$$w_k = \frac{1}{2} (D\alpha_k^2 + K_1 + K_2 + 2K_b) \quad w_0 = \frac{1}{2} (K_1 + K_2 + 2K_b) \quad (15a)$$

$$v_k = \sqrt{\frac{1}{4} (D\alpha_k^2 + K_1 + K_2)^2 - K_2 D\alpha_k^2} \quad v_0 = \frac{1}{2} (K_1 + K_2) \quad (15b)$$

one can write

$$\beta_k = w_k + v_k \quad \beta_0 = K_1 + K_2 + K_b \quad (16a)$$

$$\gamma_k = w_k - v_k \quad \gamma_0 = K_b \quad (16b)$$

The generalized solutions for f1 and c1 are:

$$f1 = \sum_{k=0}^{\infty} (A_k e^{-\beta_k t} + B_k e^{-\gamma_k t}) J_0(\alpha_k r) \quad (17a)$$

$$c1 = \sum_{k=0}^{\infty} (a_k e^{-\beta_k t} + b_k e^{-\gamma_k t}) J_0(\alpha_k r) \quad (17b)$$

The initial distribution $h(r, 0)$ must be expanded into a Bessel series.

$$h(r, 0) = \sum_{k=0}^{\infty} E_k J_0(\alpha_k r) \quad \text{bleached concentrations} \quad (18)$$

The determination of E_k can be done by the orthogonality relation:

Orthogonality

$$\int_0^{wR} r h(r, 0) J_0(\alpha_m r) dr = \int_0^{wR} \sum_{k=0}^{\infty} r E_k J_0(\alpha_k r) J_0(\alpha_m r) dr$$

$$= \frac{w^2 R^2}{2} J_0^2(\chi_m) E_m$$

Which is described in detail in appendix (A-4).

Because of $h(r, 0) \approx 0$ for $r > R$, E_k can be written as:

$$E_k = \frac{2}{w^2 R^2 J_0^2(\chi_k)} \int_0^R r h(r, 0) J_0(\alpha_k r) dr$$

(19)

The determination of A_k, B_k, a_k, b_k follows the scheme below:

$$F_{eq} = \frac{K_2}{K_1 + K_2} \quad C_{eq} = (1 - F_{eq}) = \frac{K_1}{K_1 + K_2}$$

$$f_1(r, 0) + F_{eq} = f(r, 0) = F_{eq} h(r, 0) \tag{20a}$$

$$c_1(r, 0) + C_{eq} = c(r, 0) = (1 - F_{eq}) h(r, 0) \tag{20b}$$

Equating the coefficients:

$$A_k + B_k = F_{eq} E_k \tag{21a}$$

$$a_k + b_k = (1 - F_{eq}) E_k \tag{21b}$$

$$A_0 + B_0 + F_{eq} = F_{eq} E_0 \tag{21c}$$

$$a_0 + b_0 + C_{eq} = (1 - F_{eq}) E_0 \tag{21d}$$

with (13a) and (14a)

$$A_k + B_k = F_{eq} E_k \tag{22a}$$

$$A_k \frac{K_1}{-\beta_k + K_2 + K_b} + B_k \frac{K_1}{-\gamma_k + K_2 + K_b} = (1 - F_{eq}) E_k \tag{22b}$$

$$A_0 + B_0 + F_{eq} = F_{eq} E_0 \tag{22c}$$

$$A_0 \frac{K_1}{-\beta_0 + K_2 + K_b} + B_0 \frac{K_1}{-\gamma_0 + K_2 + K_b} + C_{eq} = (1 - F_{eq}) E_0 \tag{22d}$$

The coefficients of the Bessel series (23)-(25d) follow from the equations (22a), (22b), (22c), (22d), as proven in the appendix (B-1) to (B-13).

$$(-\beta_k + K_2 + K_b)(-\gamma_k + K_2 + K_b) = -K_1 K_2 \tag{23}$$

$$A_k = -\frac{1}{2v_k} [-\beta_k + K_1 + K_2 + K_b] F_{eq} E_k \quad (24a)$$

$$B_k = \frac{1}{2v_k} [-\gamma_k + K_1 + K_2 + K_b] F_{eq} E_k \quad (24b)$$

$$A_0 = 0 \quad (24c)$$

$$B_0 = F_{eq} (E_0 - 1) \quad (24d)$$

$$a_k = \frac{1}{2v_k} [-\gamma_k + K_b] (1 - F_{eq}) E_k \quad (25a)$$

$$b_k = -\frac{1}{2v_k} [-\beta_k + K_b] (1 - F_{eq}) E_k \quad (25b)$$

$$a_0 = 0 \quad (25c)$$

$$b_0 = (1 - F_{eq}) (E_0 - 1) \quad (25d)$$

As A_0 and a_0 are zero β_0 need not to be calculated and γ_0 follows from (16b).

$$\gamma_0 = K_b \quad (26)$$

2.2 Series Expansion for the Sums of the Unbleached Concentrations $frap(r, t)$

With equation (10a),(10b),(17a) and (17b) the expansion of the Bessel series is

$$frap(r, t) = 1 - h(r, t) = -h_1(r, t) = -\sum_{k=0}^{\infty} [(A_k + a_k) e^{-\beta_k t} + (B_k + b_k) e^{-\gamma_k t}] J_0(\alpha_k r)$$

With the equations (24c),(24d) and (25c),(25d) and (16b) this series representation can be rewritten:

$$frap(r, t) = (1 - E_0) e^{-K_b t} - \sum_{k=1}^{\infty} [(A_k + a_k) e^{-\beta_k t} + (B_k + b_k) e^{-\gamma_k t}] J_0(\alpha_k r) \quad (27)$$

As shown in the appendix (C-1)-(C-4) the solution for a given and nonzero K_b differs from the solution for $K_b = 0$ simply by the factor $e^{-K_b t}$.

2.3 Approximating the Initial Distribution by Linear and Quadratic Terms

The coefficients of the Bessel series for the initial distribution $h(r, 0)$ are known from equation (19).

$$E_k = \frac{2}{w^2 R^2 J_0^2(\chi_m)} \int_0^R r h(r, 0) J_0(\alpha_k r) dr \quad k > 0$$

Assuming gaussian decay $h(r, 0)$ is modeled appropriately by

$$\begin{aligned} 0 < \theta < 1 \\ h(r, 0) &= 1 - \theta & 0 > r > x_c \\ h(r, 0) &= (1 - \theta) e^{-\frac{1}{2}\left(\frac{r-x_c}{\sigma}\right)^2} & x_c > r > R \\ h(r, 0) &= 0 & R > r \end{aligned} \quad (28)$$

Solving the equation for E_k assuming a gaussian decay for $h(r, 0)$ is not trivial. For further calculations the initial distribution is approximated by parabolic- and linear- functions. The approximation is done in five intervals:

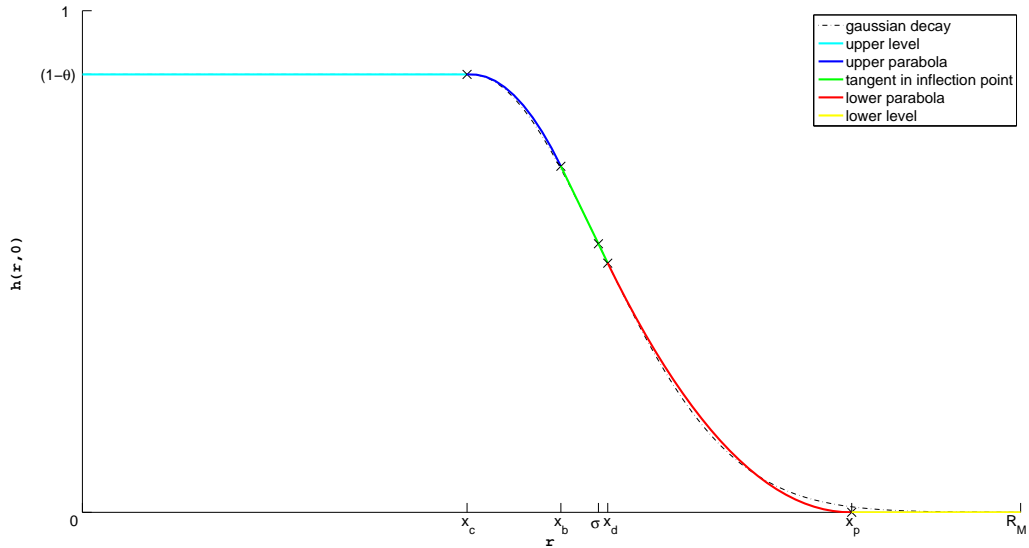


Figure 2: approximating the gaussian decay by linear and quadratic terms

$$\text{upper level :} \quad 0 > r > x_c \quad h(r, 0) = 1 - \theta \quad (29)$$

$$\text{upper parabola :} \quad x_c > r > x_b \quad h(r, 0) = (1 - \theta) \left(1 - a(r - x_c)^2\right) \quad (30)$$

$$\text{linear function :} \quad x_b > r > x_d \quad h(r, 0) = (1 - \theta) \left(\frac{1}{\sqrt{e}} - \frac{1}{\sigma\sqrt{e}}(r - (x_c + \sigma))\right) \quad (31)$$

This linear function is the tangent in the inflection point of $h(r, 0)$

$$\text{lower parabola :} \quad x_d > r > x_p \quad h(r, 0) = (1 - \theta) \left(b(r - x_p)^2\right) \quad (32)$$

$$\text{lower level :} \quad x_p > r \quad h(r, 0) = 0 \quad (33)$$

For a smooth function the gradient of the approximating function in the points x_c, x_b, x_d and x_p must be equal. With these constraints the parameters a, x_b, x_d, b, x_p can be determined. For the calculation of the these parameters the factor $(1 - \theta)$ can be left out. The gaussian function y_g that should be approximated is given:

$$\boxed{\begin{array}{ll} y_G(r) = e^{-\frac{1}{2}\left(\frac{r-x_c}{\sigma}\right)^2} & y_G(x_c + \sigma) = \frac{1}{\sqrt{e}} \\ y'_G(x_c + \sigma) = -\frac{1}{\sigma\sqrt{e}} & y''_G(x_c + \sigma) = 0 \end{array}}$$

The linear function y_t is the tangent through the inflection point $x_c + \sigma$ of the gaussian decay.

$$\boxed{y_T(r) = \frac{1}{\sqrt{e}} - \frac{1}{\sigma\sqrt{e}}(r - (x_c + \sigma)) = \frac{2}{\sqrt{e}} - \frac{1}{\sigma\sqrt{e}}(r - x_c) \quad y'_T(r) = -\frac{1}{\sigma\sqrt{e}} \quad (34)}$$

For the upper parabola the following equations lead to its parameters.

$$\begin{array}{ll} y_{uP}(r) = 1 - a(r - x_c)^2 & y'_{uP}(r) = -2a(r - x_c) \\ y_{uP}(x_b) = y_T(x_b) & y'_{uP}(x_b) = y'_T(x_b) \\ 1 - a(x_b - x_c)^2 = \frac{2}{\sqrt{e}} - \frac{1}{\sigma\sqrt{e}}(x_b - x_c) & -2a(x_b - x_c) = -\frac{1}{\sigma\sqrt{e}} \\ x_b - x_c = \frac{1}{2a\sigma\sqrt{e}} & x_b = \frac{1}{2a\sigma\sqrt{e}} + x_c \\ 1 - a\left(\frac{1}{2a\sigma\sqrt{e}}\right)^2 = \frac{2}{\sqrt{e}} - \frac{1}{\sigma\sqrt{e}}\frac{1}{2a\sigma\sqrt{e}} & \end{array}$$

Solving the system of equations for the upper parabola leads to:

$$y_{uP}(r) = 1 - a(r - x_c)^2 \quad (35a)$$

$$a = \frac{1}{4\sigma^2\sqrt{e}(2 - \sqrt{e})} \quad (35b)$$

$$x_b = 2\sigma(2 - \sqrt{e}) + x_c \quad (35c)$$

The parameter of the lower parabola are similarly determined.

$$y_{lP}(r) = b(x - x_p)^2$$

$$y'_{lP}(r) = 2b(r - x_p)$$

$$y_{lP}(x_d) = y_T(x_d)$$

$$y'_{lP}(x_d) = y'_T(x_d)$$

$$b(x_d - x_p)^2 = \frac{2}{\sqrt{e}} - \frac{1}{\sigma\sqrt{e}}(x_d - x_c)$$

$$2b(x_d - x_p) = -\frac{1}{\sigma\sqrt{e}}$$

$$x_d = \frac{1}{2b\sigma\sqrt{e}} + x_p$$

$$\frac{1}{4b\sigma^2e} = \frac{2}{\sqrt{e}} - \frac{1}{\sigma\sqrt{e}}\left(\frac{1}{2b\sigma\sqrt{e}} + x_p - x_c\right)$$

Solving the system of equations for the lower parabola leads to

$$y_{lP}(r) = b(r - x_p)^2 \quad (36a)$$

$$b = \frac{1}{4\sigma^2\sqrt{e}(x_p - 2\sigma - x_c)} \quad (36b)$$

$$x_d = 4\sigma + 2x_c - x_p \quad (36c)$$

For the calculation of E_0 and E_k the piecewise approximation leads to a piecewise integration.

For E_0 one gets:

$$E_0 = \frac{2(1 - \theta)}{w^2R^2} \left(\int_0^{x_c} r dr + \int_{x_c}^{x_b} r [1 - a(r - x_c)^2] dr + \frac{1}{\sqrt{e}} \int_{x_b}^{x_d} r \left[2 - \frac{1}{\sigma}(r - x_c) \right] dr + \int_{x_d}^{x_d} b(r - x_p)^2 r dr \right) \quad (37)$$

which results in:

$$\begin{aligned}
E_0 = \frac{2(1-\theta)}{w^2 R^2} & \left(\frac{x_c^2}{2} \right. \\
& - 1/4 a (x_b^4 - x_c^4) + 2/3 a x_c (x_b^3 - x_c^3) + 1/2 (1 - a x_c^2) (x_b^2 - x_c^2) \\
& + \frac{1}{\sqrt{e}} \left[-\frac{1/3}{\sigma} (x_d^3 - x_b^3) + 1/2 \left(1 + \frac{x_c + \sigma}{\sigma} \right) (x_d^2 - x_b^2) \right] \\
& \left. - 1/12 b (3x_d - x_p) (x_d - x_p)^3 \right) \quad (38)
\end{aligned}$$

For E_k and $k \neq 0$ the piecewise integration leads to:

$$\begin{aligned}
E_k = (1-\theta) \frac{2}{w^2 R^2 J_0(\chi_m)} & \left(\int_0^{x_c} r J_0(\alpha_k r) dr \right. \\
& + \int_{x_c}^{x_b} r \left[1 - a(r - x_c)^2 \right] J_0(\alpha_k r) dr + \frac{1}{\sqrt{e}} \int_{x_b}^{x_d} r \left[2 - \frac{1}{\sigma} (r - x_c) \right] J_0(\alpha_k r) dr \\
& \left. + \int_{x_d}^{x_d} b (r - x_p)^2 r J_0(\alpha_k r) dr \right) \quad (39)
\end{aligned}$$

For each interval the according integral is determined separately.

For the constant function:

$$I_1(X) = \int_0^X r J_0(\alpha_k r) dr$$

The following relation is found in [5]

$$\int z^{\nu+1} J_\nu(z) dz = z^{\nu+1} J_{\nu+1}(z) \quad (40)$$

$$I_1(X) = \frac{1}{\alpha_k^2} \int_0^X \alpha_k r J_0(\alpha_k r) d(\alpha_k r) = \frac{1}{\alpha_k^2} \int_0^{\alpha_k X} u J_0(u) du = \frac{1}{\alpha_k^2} \alpha_k X J_1(\alpha_k X)$$

$$\boxed{I_1(X) = \frac{X}{\alpha_k} J_1(\alpha_k X)} \quad (41)$$

For the linear approximation the solution of the following integral is needed.

$$I_2(X) = \int_0^X r^2 J_0(\alpha_k r) dr$$

The following relations [5] and [4] are used.

$$\int z^\mu J_\nu(z) dz = (\mu + \nu - 1) z J_\nu(z) S_{\mu-1, \nu-1}(z) - z J_{\nu-1}(z) S_{\mu, \nu}(z) \quad (42a)$$

$$S_{\mu, \nu}(z) = s_{\mu, \nu}(z) + 2^{\mu-1} \Gamma\left(\frac{\mu - \nu + 1}{2}\right) \Gamma\left(\frac{\mu + \nu + 1}{2}\right) \left[\sin\left(\frac{\pi\mu}{2} - \frac{\pi\nu}{2}\right) J_\nu(z) - \cos\left(\frac{\pi\mu}{2} - \frac{\pi\nu}{2}\right) Y_\nu(z) \right] \quad (42b)$$

$$s_{\mu, -\nu}(z) = s_{\mu, \nu}(z), S_{\mu, -\nu}(z) = S_{\mu, \nu}(z)$$

$$\Gamma(\alpha + 1) = \alpha \Gamma(\alpha), \Gamma(1/2) = \sqrt{\pi} \quad (42c)$$

$$s_{\mu, \nu}(z) = \frac{z^{\mu+1}}{(\mu + \nu + 1)(\mu - \nu + 1)} {}_1F_2\left(1; \frac{\mu - \nu + 3}{2}, \frac{\mu + \nu + 3}{2}; -\frac{1}{4}z^2\right) \quad (42d)$$

With these relations (42) the integral $I_2(X)$ can be written:

$$I_2(X) = \frac{1}{\alpha_k^3} \int_0^X (\alpha_k r)^2 J_0(\alpha_k r) d(\alpha_k r) = \frac{1}{\alpha_k^3} \int_0^{\alpha_k X} u^2 J_0(u) du \quad (43)$$

$$\int u^2 J_0(u) du = u J_0(u) S_{1,1}(u) + u J_1(u) S_{2,0}(u) \quad (44)$$

$$S_{1,1}(u) = s_{1,1}(u) - \frac{\pi}{2} Y_1(u) \quad (45)$$

$$S_{2,0}(u) = s_{2,0}(u) + \frac{\pi}{2} Y_0(u) \quad (46)$$

$$s_{1,1}(u) = \frac{u^2}{3} {}_1F_2\left(1; 3/2, 5/2; -1/4 u^2\right) \quad (47)$$

$$s_{2,0}(u) = \frac{u^3}{9} {}_1F_2\left(1; 5/2, 5/2; -1/4 u^2\right) \quad (48)$$

For the lower bound of the definite integral the following limit has to be considered:

$$\lim_{u \rightarrow 0} \left[\underbrace{u J_0(u) S_{1,1}(u)}_{+1} + \underbrace{u J_1(u) S_{2,0}(u)}_0 \right] = 1$$

Therefore $I_2(X)$ is given:

$$\boxed{I_2(X) = \int_0^X r^2 J_0(\alpha_k r) dr = \frac{1}{\alpha_k^3} \left[\alpha_k X J_0(\alpha_k X) S_{1,1}(\alpha_k X) - \alpha_k X J_1(\alpha_k X) S_{2,0}(\alpha_k X) - 1 \right]} \quad (49)$$

The parabolic approximation leads to the integral:

$$I_3(X) = \int_0^X r^3 J_0(\alpha_k r) dr$$

$$I_3(X) = \frac{1}{\alpha_k^4} \int_0^X (\alpha_k r)^3 J_0(\alpha_k r) d(\alpha_k r) = \frac{1}{\alpha_k^4} \int_0^{\alpha_k X} u^3 J_0(u) du$$

$$\int z^{\nu+1} J_\nu(z) dz = z^{\nu+1} J_{\nu+1}(z)$$

Integrating by parts and observing the relations above from [5] one can proceed to:

$$\int u^3 J_0(u) du = \int u^2 (u J_0(u)) du$$

$$\int u^3 J_0(u) du = u^3 J_1(u) - 2u^2 J_2(u)$$

$$I_3(X) = \int_0^X r^3 J_0(\alpha_k r) dr = \frac{X^2}{\alpha_k^2} [\alpha_k X J_1(\alpha_k X) - 2J_2(\alpha_k X)] \quad (50)$$

The coefficients of the Bessel series by the approximated initial distribution with (41), (49), (50) and (19) are

$$E_k = (1 - \theta) \frac{2}{w^2 R^2 J_0^2(\chi_m)} \left(I_1(x_c) \right. \\ \left. - a(I_3(x_b) - I_3(x_c)) + 2ax_c(I_2(x_b) - I_2(x_c)) + (1 - ax_c^2)(I_1(x_b) - I_1(x_c)) \right. \\ \left. - \frac{1}{\sigma\sqrt{e}}(I_2(x_d) - I_2(x_b)) + \frac{(2 + \frac{1}{\sigma}x_c)}{\sqrt{e}}(I_1(x_d) - I_1(x_b)) \right. \\ \left. - b(I_3(x_p) - I_2(x_d)) - 2bx_p(I_2(x_p) - I_2(x_d)) + bx_p^2(I_1(x_p) - I_1(x_d)) \right) \quad (51)$$

The calculation of the integral I_2 (49) is the bottleneck of this Bessel series expansion. With greater k 's the numeric implementation of the hypergeometric function ${}_1F_2$ in Matlab can lead to a deadlock. Consequently the hypergeometric function is used element-wise in order to compute the Bessel series expansion of the integral. This is done in a try-catch-block to calculate up to the maximal possible term number.

2.4 Set of Analytical Formulas for the Forward Problem

The measured FRAP date of one time stamp is the sum of free and bound fluorescence, averaged over the bleach spot [9]. Actually $frap(r, t)$ is the average over φ of $f\widetilde{rap}(r, \varphi, t)$, which is assumed to be rotationally symmetric. The $Frap(t)$ is the average of the $frap(r, t)$ over the whole spot area.

$$\begin{aligned} Frap(t) &= \frac{1}{\pi R^2} \int_0^R \int_0^{2\pi} frap(r, t) r d\varphi dr = \frac{2\pi}{\pi R^2} \int_0^R r frap(r, t) dr \\ &= \frac{2}{R^2} \int_0^R r \left[(1 - E_0) e^{-K_b t} \right. \\ &\quad \left. - \sum_{k=1}^{\infty} \left[(A_k + a_k) e^{-\beta_k t} + (B_k + b_k) e^{-\gamma_k t} \right] J_0(\alpha_k r) \right] dr \\ &= (1 - E_0) e^{-K_b t} - \frac{1}{R^2} \sum_{k=1}^{\infty} \left[(A_k + a_k) e^{-\beta_k t} + (B_k + b_k) e^{-\gamma_k t} \right] \int_0^R r J_0(\alpha_k r) dr \end{aligned}$$

and with equation (41) the FRAP representation can be written

$$Frap(t) = (1 - E_0) e^{-K_b t} - \frac{2}{R^2} \sum_{k=1}^{\infty} \left[(A_k + a_k) e^{-\beta_k t} + (B_k + b_k) e^{-\gamma_k t} \right] \frac{R J_1(\alpha_k w R)}{\alpha_k} \quad (52)$$

With the equations (12), (24a), (25a) and (21c) the complete set of formulas for calculating the Frap function depending on the parameter K_1, K_2, D is given:

$w_k = 1/2 \left(D\alpha_k^2 + K_1 + K_2 + 2K_b \right)$	
$v_k = \sqrt{1/4 \left(D\alpha_k^2 K_1 K_2 \right)^2 - K_2 D\alpha_k^2}$	
$\beta_k = w_k + v_k$	
$\gamma_k = w_k - v_k$	
$AA_k = A_k + a_k = \frac{E_k}{2v_k} \left[\beta_k F_{eq} - \gamma_k (1 - F_{eq}) - (2F_{eq} - 1) K_b - K_2 \right]$	(53)
$BB_k = E_k - AA_k \quad \text{from} \quad E_k = A_k + a_k + B_k + b_k$	(54)
$Frap(t) = (1 - E_0) e^{-K_b t} - 2w \sum_{k=1}^{\infty} \left(AA_k e^{-\beta_k t} + BB_k e^{-\gamma_k t} \right) \frac{J_1(\alpha_k R)}{\chi_k}$	(55)

2.5 Parameter Estimation

The FRAP model is a nonlinear system to the parameters K_1, K_2 and D . To solve this inverse problem in order to estimate the parameters from given data, the weighted least

square [WLS] method with the Gauss-Newton iteration step update is implemented [2].

$$\mathbf{p} = \begin{bmatrix} K_1 \\ K_2 \\ D \end{bmatrix} \quad (56)$$

The weights of the estimator are defined by the variance of the data, or the identity matrix.

$$\mathbf{W} = \begin{bmatrix} \sigma_1^{-2} & \dots & 0 \\ \vdots & \ddots & \vdots \\ 0 & \dots & \sigma_T^{-2} \end{bmatrix} \quad (57)$$

The goal is to minimize for measured FRAP data iteratively the cost function C with respect to \mathbf{p} :

$$C = \|\mathbf{FRAP} - \mathbf{Frap}(\mathbf{p})\|_{\mathbf{W}}^2 = \frac{1}{2} [\mathbf{FRAP} - \mathbf{Frap}(\mathbf{p})]^T \mathbf{W} [\mathbf{FRAP} - \mathbf{Frap}(\mathbf{p})] \quad (58)$$

$$\frac{\partial C}{\partial \mathbf{p}} = \nabla C = 0 \quad \frac{\partial^2 C}{\partial \mathbf{p}^2} = \mathbf{H}_C(\mathbf{p}) \quad \text{positive definite} \quad (59)$$

For the weighted least square estimator the gradient of C is developed into a Taylor series up to the linear term. The linearization is set to zero in every iteration step.

$$\hat{\mathbf{p}} = \arg \min_{\mathbf{p}} C = \arg \min_{\mathbf{p}} \frac{1}{2} [\mathbf{FRAP} - \mathbf{Frap}(\mathbf{p})]^T \mathbf{W} [\mathbf{FRAP} - \mathbf{Frap}(\mathbf{p})] \quad (60)$$

$$\nabla C(\mathbf{p}_0 + \Delta \mathbf{p}) = \nabla C(\mathbf{p}_0) + \mathbf{H}_C(\mathbf{p}_0) \Delta \mathbf{p} \stackrel{!}{=} 0 \quad \text{expansion around } \mathbf{p}_0 \quad (61)$$

$$\Delta \mathbf{p} = -\mathbf{H}_C(\mathbf{p}_0)^{-1} \nabla C(\mathbf{p}_0) \quad (62)$$

$$\nabla C(\mathbf{p}_0) = -\mathbf{S}^T \mathbf{W} [\mathbf{FRAP} - \mathbf{Frap}(\mathbf{p}_0)] \quad (63)$$

$$\mathbf{H}_C(\mathbf{p}_0) = \mathbf{S}^T \mathbf{W} \mathbf{S} - \sum_{k=1}^T \mathbf{Hess}(\mathbf{Frap}_k(\mathbf{p}_0)) \frac{1}{\sigma_k^2} (\mathbf{FRAP}_k - \mathbf{Frap}_k(\mathbf{p}_0)) \quad (64)$$

For the Hessian H_c the second term can be omitted, as near a minimum the residuals tends rapidly towards zero. So the iteration step in the parameter space is approximately

$$\Delta \mathbf{p} = \left(\mathbf{S}^T \mathbf{W} \mathbf{S} \right)^{-1} \mathbf{S}^T \mathbf{W} [\mathbf{FRAP} - \mathbf{Frap}(\mathbf{p})] \quad (65)$$

2.6 Set of Analytical Formulas for the Inverse Problem

Performing the weighted least square algorithm with Gauss-Newton iteration the sensitivity matrix S , which is the Jacobian of \mathbf{Frap} with respect to \mathbf{p} , has to be found. Another method for parameter identification is to apply the Matlab built-in solver. The Jacobian and the Hessian of the residuals can optionally be handed over to the solver. So the second

partial derivatives of the FRAP model also have to be assembled. For further calculations a rearranged Hessian is introduced, this matrix has the same elements as the intrinsically three dimensional Jacobian of the Sensitivity but is rearranged into two dimensions. The sensitivity matrix \mathbf{S} and this rearranged matrix \mathbf{rH} are defined as

$$\mathbf{S} = \begin{bmatrix} \frac{\partial \mathbf{Frap}}{\partial K_1} & \frac{\partial \mathbf{Frap}}{\partial K_2} & \frac{\partial \mathbf{Frap}}{\partial D} \end{bmatrix} \quad (66)$$

$$\begin{aligned} \mathbf{rH} &= \begin{bmatrix} \frac{\partial \mathbf{S}}{\partial K_1} & \frac{\partial \mathbf{S}}{\partial K_2} & \frac{\partial \mathbf{S}}{\partial D} \end{bmatrix} \\ &= \begin{bmatrix} \frac{\partial^2 \mathbf{Frap}}{\partial K_1^2} & \frac{\partial^2 \mathbf{Frap}}{\partial K_1 \partial K_2} & \frac{\partial^2 \mathbf{Frap}}{\partial K_1 \partial D} & \frac{\partial^2 \mathbf{Frap}}{\partial K_2 \partial K_1} & \frac{\partial^2 \mathbf{Frap}}{\partial K_2^2} & \frac{\partial^2 \mathbf{Frap}}{\partial K_2 \partial D} & \frac{\partial^2 \mathbf{Frap}}{\partial D \partial K_1} & \frac{\partial^2 \mathbf{Frap}}{\partial D \partial K_2} & \frac{\partial^2 \mathbf{Frap}}{\partial D^2} \end{bmatrix} \end{aligned} \quad (67)$$

Observing the results derived in section 2.4 the differentiation with respect to K_1, K_2 and D leads to

$$\frac{\partial w_k}{\partial K_1} = \frac{\partial w_k}{\partial K_2} = \frac{1}{2} \quad (68)$$

$$\frac{\partial w_k}{\partial D} = \frac{1}{2} \alpha_k^2 \quad (69)$$

$$\frac{\partial^2 w_k}{\partial K_1^2} = \frac{\partial^2 w_k}{\partial K_1 \partial K_2} = \frac{\partial^2 w_k}{\partial K_1 \partial D} = \frac{\partial^2 w_k}{\partial K_2^2} = \frac{\partial^2 w_k}{\partial K_2 \partial D} = \frac{\partial^2 w_k}{\partial D^2} = 0 \quad (70)$$

$$\frac{\partial v_k}{\partial K_1} = \frac{1}{4v_k} (D\alpha_k^2 + K_1 + K_2) \quad (71)$$

$$\frac{\partial v_k}{\partial K_2} = \frac{1}{4v_k} (-D\alpha_k^2 + K_1 + K_2) \quad (72)$$

$$\frac{\partial v_k}{\partial D} = \frac{1}{4v_k} \alpha_k^2 (D\alpha_k^2 + K_1 - K_2) \quad (73)$$

$$\frac{\partial^2 v_k}{\partial K_1^2} = -\frac{K_2 D \alpha_k^2}{4v_k^3} \quad (74)$$

$$\frac{\partial^2 v_k}{\partial K_1 \partial K_2} = \frac{D \alpha_k^2}{8v_k^3} (D\alpha_k^2 + K_1 - K_2) \quad (75)$$

$$\frac{\partial^2 v_k}{\partial K_1 \partial D} = \frac{K_2 \alpha_k^2}{8v_k^3} (-D\alpha_k^2 + K_1 + K_2) \quad (76)$$

$$\frac{\partial^2 v_k}{\partial K_2^2} = \frac{K_1 D \alpha_k^2}{4v_k^3} \quad (77)$$

$$\frac{\partial^2 v_k}{\partial K_2 \partial D} = -\frac{K_1 \alpha_k^2}{8v_k^3} (D\alpha_k^2 + K_1 + K_2) \quad (78)$$

$$\frac{\partial^2 v_k}{\partial D^2} = \frac{K_1 K_2 \alpha_k^2}{4v_k^3} \quad (79)$$

$$\frac{\partial \beta_k}{\partial p} = \frac{\partial v_k}{\partial p} + \frac{\partial w_k}{\partial p} \quad (80)$$

$$\frac{\partial^2 \beta_k}{\partial p^2} = \frac{\partial^2 v_k}{\partial p^2} + \frac{\partial^2 w_k}{\partial p^2} \quad (81)$$

$$\frac{\partial^2 \beta_k}{\partial p_1 \partial p_2} = \frac{\partial^2 v_k}{\partial p_1 \partial p_2} + \frac{\partial^2 w_k}{\partial p_1 \partial p_2} \quad (82)$$

The detailed set of derivatives of β can be found in appendix A.4 equations (D-1)-(D-9). The partial derivatives of γ_k could be constructed in a similar way observing that $\gamma_k = v_k - w_k$. As numerical subtraction of values of the same order of magnitude means loss of accuracy, γ_k is expressed for numerical optimization by

$$\gamma_k = \frac{Z_k}{\beta_k} \quad (83)$$

$$Z_k = (K_b + K_2) D \alpha_k^2 + K_b (K_b + K_1 + K_2) \quad (84)$$

So the partial derivatives of Z are needed as well

$$\frac{\partial Z_k}{\partial K_1} = K_b \quad (85)$$

$$\frac{\partial Z_k}{\partial K_2} = D \alpha_k^2 + K_b \quad (86)$$

$$\frac{\partial Z_k}{\partial D} = (K_b + K_2) \alpha_k^2 \quad (87)$$

$$\frac{\partial^2 Z_k}{\partial K_2 \partial D} = \alpha_k^2 \quad (88)$$

$$\frac{\partial^2 Z_k}{\partial K_1^2} = \frac{\partial^2 Z_k}{\partial K_1 \partial K_2} = \frac{\partial^2 Z_k}{\partial K_1 \partial D} = \frac{\partial^2 Z_k}{\partial K_2^2} = \frac{\partial^2 Z_k}{\partial D^2} = 0 \quad (89)$$

The derivatives of γ_k are assembled by the quotient rule and the second derivatives are simplified by (89) to

$$\frac{\partial \gamma_k}{\partial p} = \frac{1}{\beta_k^2} \left(\frac{\partial Z_k}{\partial p} \beta_k - \frac{\partial \beta_k}{\partial p} Z_k \right) \quad (90)$$

$$\frac{\partial^2 \gamma_k}{\partial p^2} = \frac{1}{\beta_k^3} \left(\beta_k \left(-2 \frac{\partial \beta_k}{\partial p} \frac{\partial Z_k}{\partial p} - \frac{\partial^2 \beta_k}{\partial p^2} Z_k \right) + 2 \frac{\partial \beta_k^2}{\partial p} Z_k \right) \quad (91)$$

The set of partial derivatives of γ can be found in appendix A.4 equations (D-10)-(D-15).

$$\frac{\partial^2 \gamma_k}{\partial K_1 \partial K_2} = \frac{1}{\beta_k^3} \left(\beta_k \left(\frac{\partial \beta_k}{\partial K_2} \frac{\partial Z_k}{\partial K_1} - \frac{\partial \beta_k}{\partial K_1} \frac{\partial Z_k}{\partial K_2} - \frac{\partial^2 \beta_k}{\partial K_1 \partial K_2} Z_k \right) + 2 \frac{\partial \beta_k}{\partial K_1} \frac{\partial \beta_k}{\partial K_2} Z_k \right) \quad (92)$$

$$\frac{\partial^2 \gamma_k}{\partial K_1 \partial D} = \frac{1}{\beta_k^3} \left(\beta_k \left(-\frac{\partial \beta_k}{\partial D} \frac{\partial Z_k}{\partial K_1} - \frac{\partial \beta_k}{\partial K_1} \frac{\partial Z_k}{\partial D} - \frac{\partial^2 \beta_k}{\partial K_1 \partial D} Z_k \right) + 2 \frac{\partial \beta_k}{\partial K_1} \frac{\partial \beta_k}{\partial D} Z_k \right) \quad (93)$$

$$\frac{\partial^2 \gamma_k}{\partial K_2 \partial D} = \frac{1}{\beta_k^3} \left(\beta_k \left(\frac{\partial^2 Z_k}{\partial K_2 \partial D} \beta_k - \frac{\partial \beta_k}{\partial D} \frac{\partial Z_k}{\partial K_2} - \frac{\partial \beta_k}{\partial K_2} \frac{\partial Z_k}{\partial D} - \frac{\partial^2 \beta_k}{\partial K_2 \partial D} Z_k \right) + 2 \frac{\partial \beta_k}{\partial K_2} \frac{\partial \beta_k}{\partial D} Z_k \right) \quad (94)$$

The derivatives of AA_k are

$$\frac{\partial AA_k}{\partial K_1} = \frac{K_2 D^2 \alpha_k^4 E_k}{8v_k^3 (K_1 + K_2)^2} \left(-K_2 + D\alpha_k^2 + 3K_1 \right) \quad (95)$$

$$\frac{\partial AA_k}{\partial K_2} = \frac{K_1 D^2 \alpha_k^4 E_k}{8v_k^3 (K_1 + K_2)^2} \left(K_1 - 3K_2 + D\alpha_k^2 \right) \quad (96)$$

$$\frac{\partial AA_k}{\partial D} = \frac{K_1 K_2 D \alpha_k^4 E_k}{4v_k^3 (K_1 + K_2)} \quad (97)$$

$$\begin{aligned} \frac{\partial^2 AA_k}{\partial K_1^2} = \frac{K_2 D^2 \alpha_k^4 E_k}{16v_k^5 (K_1 + K_2)^3} & \left(5K_1 D^2 \alpha_k^4 + 6K_2^2 D^2 \alpha_k^4 + 10K_1^2 D \alpha_k^2 + D^3 \alpha_k^6 \right. \\ & \left. - 4K_2^3 + 6K_1^3 - 2K_1 K_2^2 + 8K_1^2 K_2 \right) \quad (98) \end{aligned}$$

$$\begin{aligned} \frac{\partial^2 AA_k}{\partial K_1 \partial K_2} = -\frac{D^2 \alpha_k^4 E_k}{32v_k^5 (K_1 + K_2)^3} & \left(-7K_2^3 D \alpha_k^2 + 7K_1^3 D \alpha_k^2 + 5K_2^2 D^2 \alpha_k^4 \right. \\ & + 5K_1^2 D^2 \alpha_k^4 - K_2 D^3 \alpha_k^6 + K_1 D^3 \alpha_k^6 - 8K_1 K_2^3 \\ & - 6K_1 K_2 D^2 \alpha_k^4 + 9K_1 K_2^2 D \alpha_k^2 - 9K_1^2 K_2 D \alpha_k^2 \\ & \left. + 3K_1^4 - 22K_1^2 K_2^2 - 8K_1^3 K_2 + 3K_2^4 \right) \quad (99) \end{aligned}$$

$$\begin{aligned} \frac{\partial^2 AA_k}{\partial K_1 \partial D} = -\frac{K_2 D^2 \alpha_k^4 E_k}{16v_k^5 (K_1 + K_2)^2} & \left(-K_2 D^2 \alpha_k^4 + 3K_1^2 D \alpha_k^2 + K_1 K_2 D \alpha_k^2 \right. \\ & \left. + 2K_2^2 D \alpha_k^2 + 5K_1^2 K_2 + K_1 K_2^2 - K_2^3 + 3K_1^3 \right) \quad (100) \end{aligned}$$

$$\begin{aligned} \frac{\partial^2 AA_k}{\partial K_2^2} = -\frac{K_1 D^2 \alpha_k^4 E_k}{16v_k^5 (K_1 + K_2)^3} & \left(10K_2^2 D \alpha_k^2 - 5K_2 D^2 \alpha_k^4 - 8K_1 K_2^2 + 3K_1 D^2 \alpha_k^4 \right. \\ & \left. + 2K_1^2 K_2 + 6K_1^2 D \alpha_k^2 - 6K_2^3 + 4K_1^3 + D^3 \alpha_k^6 \right) \quad (101) \end{aligned}$$

$$\begin{aligned} \frac{\partial^2 AA_k}{\partial K_2 \partial D} = \frac{K_D \alpha_k^4 E_k}{16v_k^5 (K_1 + K_2)^2} & \left(K_1 D^2 \alpha_k^4 + 2K_1^2 D \alpha_k^2 + K_1 K_2 D \alpha_k^2 + K_1^3 \right. \\ & \left. - K_1^2 K_2 - 5K_1 K_2^2 + 3K_2^2 D \alpha_k^2 - 3K_2^3 \right) \quad (102) \end{aligned}$$

$$\frac{\partial^2 AA_k}{\partial D^2} = \frac{K_1 K_2 \alpha_k^4 E_k}{16v_k^5 (K_1 + K_2)} \left(-2D^2 \alpha_k^2 - K_1 D \alpha_k^2 + K_2 D \alpha_k^2 + K_1^2 + 2K_1 K_2 + K_2^2 \right) \quad (103)$$

All this partial derivatives were developed by the Matlab symbolic toolbox. A short description of the usage and an example is found in appendix A.5.

The derivatives of the exponential function are given

$$\frac{\partial e^{-ft}}{\partial p} = -t \frac{\partial f}{\partial p} e^{-ft} \quad (104)$$

$$\begin{aligned} \frac{\partial^2 e^{-ft}}{\partial p_1 \partial p_2} &= -t \frac{\partial^2 f}{\partial p_1 \partial p_2} e^{-ft} - t \frac{\partial f}{\partial p_1} \frac{\partial e^{-ft}}{\partial p_2} \\ \frac{\partial^2 e^{-ft}}{\partial p_1 \partial p_2} &= -t \frac{\partial^2 f}{\partial p_1 \partial p_2} e^{-ft} + t^2 \frac{\partial f}{\partial p_1} \frac{\partial f}{\partial p_2} e^{-ft} \end{aligned} \quad (105)$$

Substituting γ_k, β_k for $f(p)$ provides the derivatives, shown in appendix (D-16)-(D-25) and (D-26)-(D-35). Applying the chain rule for the elements of the sensitivity matrix S with equation (55):

$$\begin{aligned} \frac{\partial Frap}{\partial p} &= -2w \sum_{k=1}^{\infty} \left(\frac{\partial AA_k}{\partial p} e^{-\beta_k t} + AA_k \frac{\partial e^{-\beta_k t}}{\partial p} \right. \\ &\quad \left. - \frac{\partial AA_k}{\partial p} e^{-\gamma_k t} + (E_k - AA_k) \frac{\partial e^{-\gamma_k t}}{\partial p} \right) \frac{J_1(\alpha_k R)}{\chi_k} \end{aligned} \quad (106)$$

For one element of the Hessian the general formulation is

$$\begin{aligned} \frac{\partial^2 Frap}{\partial p_1 \partial p_2} &= -2w \sum_{k=1}^{\infty} \left(\frac{\partial^2 AA_k}{\partial p_1 \partial p_2} e^{-\beta_k t} + \frac{\partial AA_k}{\partial p_1} \frac{\partial e^{-\beta_k t}}{\partial p_2} \right. \\ &\quad + \frac{\partial AA_k}{\partial p_2} \frac{\partial e^{-\beta_k t}}{\partial p_1} + AA_k \frac{\partial^2 e^{-\beta_k t}}{\partial p_1 \partial p_2} - \frac{\partial^2 AA_k}{\partial p_1 \partial p_2} e^{-\gamma_k t} - \frac{\partial AA_k}{\partial p_1} \frac{\partial e^{-\gamma_k t}}{\partial p_2} \\ &\quad \left. - \frac{\partial AA_k}{\partial p_2} \frac{\partial e^{-\gamma_k t}}{\partial p_1} + (E_k - AA_k) \frac{\partial^2 e^{-\gamma_k t}}{\partial p_1 \partial p_2} \right) \frac{J_1(\alpha_k R)}{\chi_k} \end{aligned} \quad (107)$$

Substituting the derivatives (106) and (107) in S (66) and rH (67) the set of formulas for numerical processing is achieved.

2.7 Numerical Representation of $Frap(t)$

The numerical implementation of $Frap(t)$ equation (55) with K Bessel terms for T time stamps of the measurement is shown in the following section. As the main strength of Matlab is effective matrix calculation and manipulation, the formulations are constructed with regard to the special abilities of this programming tool. The $Frap$ (sum over K Bessel terms) is provided by a matrix multiplication, leading to a column matrix for $Frap$.

```
Frap=( (1-E0)*exp(-Kb*td)-2*w*((AA.*J1wxi)'*eea+(E-AA).*J1wxi)'*eeb)';
```

with the definitions

$$\begin{aligned}
\mathbf{t} &= [t_1 \quad \dots \quad t_T] \\
\mathbf{AA} &= [AA_1 \quad \dots \quad AA_K]^\top \\
\mathbf{E} &= [E_1 \quad \dots \quad E_K]^\top \\
\mathbf{J1wxi} &= \left[\frac{J_1(\frac{\chi_1}{w})}{\chi_1} \quad \dots \quad \frac{J_1(\frac{\chi_K}{w})}{\chi_K} \right]^\top \\
\mathbf{eea} &= \begin{bmatrix} e^{-\beta_1 t_1} & \dots & e^{-\beta_1 t_T} \\ \vdots & \ddots & \vdots \\ e^{-\beta_K t_1} & \dots & e^{-\beta_K t_T} \end{bmatrix} \\
\mathbf{eeb} &= \begin{bmatrix} e^{-\gamma_1 t_1} & \dots & e^{-\gamma_1 t_T} \\ \vdots & \ddots & \vdots \\ e^{-\gamma_K t_1} & \dots & e^{-\gamma_K t_T} \end{bmatrix} \\
\mathbf{Frap} &= [Frap(t_1) \quad \dots \quad Frap(t_T)]^\top \\
E_0, w, K_b & \quad \dots \quad \text{scalars}
\end{aligned}$$

$$\mathbf{Frap} = \left[(1 - E_0) e^{-K_b t} - 2w \left((\mathbf{AA} .* \mathbf{J1wxi})^\top \mathbf{eea} + ((\mathbf{E} - \mathbf{AA}) .* \mathbf{J1wxi})^\top \mathbf{eeb} \right) \right]^\top$$

Shown “.*” defines a element wise matrix multiplication.

2.8 Set of Numerical Formulae for the Inverse Problem

The implementation of \mathbf{S} and the \mathbf{rH} is a straight-forward implementation of the formulas of section 2.6. For better understanding of the source code exceptions are demonstrated. For the sensitivity matrix \mathbf{S} the partial derivatives of the $Frap$ are calculated.

$$\mathbf{S} = [\mathbf{FrapK1} \quad \mathbf{FrapK2} \quad \mathbf{FrapD}] \tag{108}$$

$\mathbf{FrapK1}, \mathbf{FrapK2}, \mathbf{FrapD} \quad \dots \quad \text{derivatives of Frap}$

The derivatives for the \mathbf{S} are provided by simple matrix multiplication similar to section 2.7 .

```

FrapK1=(-2*w*((AAK1*J1wxi) .* eea+((-AAK1) .* J1wxi) .* eeb+...
(AA .* J1wxi) .* eeaK1+((E-AA) .* J1wxi) .* eebK1))';

```

With the definitions

$$\begin{aligned}
\mathbf{AAK1} &= \left[\frac{\partial AA_1}{\partial K_1} \quad \dots \quad \frac{\partial AA_K}{\partial K_1} \right]^\top \\
\mathbf{eeaK1} &= \begin{bmatrix} \frac{\partial e^{-\beta_1 t_1}}{\partial K_1} & \dots & \frac{\partial e^{-\beta_1 t_T}}{\partial K_1} \\ \vdots & \ddots & \vdots \\ \frac{\partial e^{-\beta_K t_1}}{\partial K_1} & \dots & \frac{\partial e^{-\beta_K t_T}}{\partial K_1} \end{bmatrix} \\
\mathbf{eebK1} &= \begin{bmatrix} \frac{\partial e^{-\gamma_1 t_1}}{\partial K_1} & \dots & \frac{\partial e^{-\gamma_1 t_T}}{\partial K_1} \\ \vdots & \ddots & \vdots \\ \frac{\partial e^{-\gamma_K t_1}}{\partial K_1} & \dots & \frac{\partial e^{-\gamma_K t_T}}{\partial K_1} \end{bmatrix} \\
\mathbf{FrapK1} &= \left[\frac{\partial Frap(t_1)}{\partial K_1} \quad \dots \quad \frac{\partial Frap(t_T)}{\partial K_1} \right]^\top
\end{aligned}$$

$$\begin{aligned}
\mathbf{FrapK1} &= -2w \left[\left((\mathbf{AAK1} .* \mathbf{J1wxi})^\top \mathbf{eea} + (\mathbf{AA} .* \mathbf{J1wxi})^\top \mathbf{eeaK1} \right. \right. \\
&\quad \left. \left. - (\mathbf{AAK1} .* \mathbf{J1wxi})^\top \mathbf{eeb} + ((\mathbf{E} - \mathbf{AA}) .* \mathbf{J1wxi})^\top \mathbf{eebK1} \right) \right]^\top \quad (109)
\end{aligned}$$

For the partial derivatives $\mathbf{eeaK1}, \mathbf{eebK1}$ one may write the matrix notation

$$\mathbf{eeaK1} = -\mathbf{d_betK1} \mathbf{eea} \mathbf{d_t} \quad (110)$$

$$\mathbf{eebK1} = -\mathbf{d_gamK1} \mathbf{eeb} \mathbf{d_t} \quad (111)$$

With the definitions

$$\begin{aligned}
\mathbf{d_t} &= \begin{bmatrix} t_1 & 0 & \dots & 0 \\ 0 & t_2 & \dots & 0 \\ \vdots & \vdots & \ddots & \vdots \\ 0 & 0 & \dots & t_T \end{bmatrix} \\
\mathbf{d_betK1} &= \begin{bmatrix} \frac{\partial \beta_1}{\partial K_1} & 0 & \dots & 0 \\ 0 & \frac{\partial \beta_2}{\partial K_1} & \dots & 0 \\ \vdots & \vdots & \ddots & \vdots \\ 0 & 0 & \dots & \frac{\partial \beta_K}{\partial K_1} \end{bmatrix} \\
\mathbf{d_gamK1} &= \begin{bmatrix} \frac{\partial \gamma_1}{\partial K_1} & 0 & \dots & 0 \\ 0 & \frac{\partial \gamma_2}{\partial K_1} & \dots & 0 \\ \vdots & \vdots & \ddots & \vdots \\ 0 & 0 & \dots & \frac{\partial \gamma_K}{\partial K_1} \end{bmatrix}
\end{aligned}$$

The diagonal matrices are implemented in *sparse* mode, as the sparse-multiplication leads to a lower memory and time consumption. For \mathbf{rH} the element-wise representation is

provided by

$$\mathbf{rH} = [\mathbf{FrapK1K1} \ \mathbf{FrapK1K2} \ \mathbf{FrapK1D} \ \mathbf{FrapK1K2} \dots \\ \mathbf{FrapK2K2} \ \mathbf{FrapK2D} \ \mathbf{FrapK1D} \ \mathbf{FrapK2D} \ \mathbf{FrapDD}] \quad (112)$$

$\mathbf{FrapK1K1}, \mathbf{FrapK1K2}, \text{etc.}$... second derivatives of Frap

The Matlab code for one element of \mathbf{rH} is written

```
FrapK1K2=(-2*w*((AAK1K2.*J1wxi)'*eea+(AAK1.*J1wxi)'*eeaK2...
+((-AAK1K2).*J1wxi)'*eeb+((-AAK1).*J1wxi)'*eebK2...
+(AAK2.*J1wxi)'*eeaK1+(AA.*J1wxi)'*eeaK1K2...
+((-AAK2).*J1wxi)'*eebK1+(E-AA).*J1wxi)'*eebK1K2))';
```

with the definitions

$$\mathbf{AAK1K2} = \begin{bmatrix} \frac{\partial^2 AA_1}{\partial K_1 \partial K_2} & \dots & \frac{\partial^2 AA_K}{\partial K_1 \partial K_2} \end{bmatrix}^\top$$

$$\mathbf{eeaK1K2} = \begin{bmatrix} \frac{\partial^2 e^{-\beta_1 t_1}}{\partial K_1 \partial K_2} & \dots & \frac{\partial^2 e^{-\beta_1 t_T}}{\partial K_1 \partial K_2} \\ \vdots & \ddots & \vdots \\ \frac{\partial^2 e^{-\beta_K t_1}}{\partial K_1 \partial K_2} & \dots & \frac{\partial^2 e^{-\beta_K t_T}}{\partial K_1 \partial K_2} \end{bmatrix}$$

$$\mathbf{eebK1K2} = \begin{bmatrix} \frac{\partial^2 e^{-\gamma_1 t_1}}{\partial K_1 \partial K_2} & \dots & \frac{\partial^2 e^{-\gamma_1 t_T}}{\partial K_1 \partial K_2} \\ \vdots & \ddots & \vdots \\ \frac{\partial^2 e^{-\gamma_K t_1}}{\partial K_1 \partial K_2} & \dots & \frac{\partial^2 e^{-\gamma_K t_T}}{\partial K_1 \partial K_2} \end{bmatrix}$$

$$\mathbf{FrapK1K2} = \begin{bmatrix} \frac{\partial^2 \text{Frap}(t_1)}{\partial K_1 \partial K_2} & \dots & \frac{\partial^2 \text{Frap}(t_T)}{\partial K_1 \partial K_2} \end{bmatrix}^\top$$

The representation for one element of the \mathbf{rH} by matrix multiplication is:

$$\mathbf{FrapK1K2} = -2w \left[\left((\mathbf{AAK1K2} \cdot \mathbf{J1wxi})^\top \mathbf{eea} + (\mathbf{AAK1} \cdot \mathbf{J1wxi})^\top \mathbf{eeaK1} \right. \right. \\ \left. \left. + (\mathbf{AAK2} \cdot \mathbf{J1wxi})^\top \mathbf{eeaK1} + (\mathbf{AA} \cdot \mathbf{J1wxi})^\top \mathbf{eeaK1K2} \right. \right. \\ \left. \left. - (\mathbf{AAK1K2} \cdot \mathbf{J1wxi})^\top \mathbf{eeb} - (\mathbf{AAK1} \cdot \mathbf{J1wxi})^\top \mathbf{eebK2} \right. \right. \\ \left. \left. - (\mathbf{AAK2} \cdot \mathbf{J1wxi})^\top \mathbf{eebK1} + ((\mathbf{E} - \mathbf{AA}) \cdot \mathbf{J1wxi})^\top \mathbf{eebK1K2} \right) \right]^\top \quad (113)$$

For the partial derivatives $\mathbf{eeaK1K2}, \mathbf{eebK1K2}$ the matrix notation is

$$\mathbf{eeaK1K2} = -d_betK1K2 \ \mathbf{eea} \ d_t - d_betK1 \ \mathbf{eeaK2} \ d_t \quad (114)$$

$$\mathbf{eebK1K2} = -d_gamK1K2 \ \mathbf{eeb} \ d_t - d_gamK1 \ \mathbf{eebK2} \ d_t \quad (115)$$

with the definitions

$$\begin{aligned}
 d_betK1K2 &= \begin{bmatrix} \frac{\partial^2 \beta_1}{\partial K_1 \partial K_2} & 0 & \dots & 0 \\ 0 & \frac{\partial^2 \beta_2}{\partial K_1 \partial K_2} & \dots & 0 \\ \vdots & \vdots & \ddots & \vdots \\ 0 & 0 & \dots & \frac{\partial^2 \beta_K}{\partial K_1 \partial K_2} \end{bmatrix} \\
 d_gamK1K2 &= \begin{bmatrix} \frac{\partial^2 \gamma_1}{\partial K_1 \partial K_2} & 0 & \dots & 0 \\ 0 & \frac{\partial^2 \gamma_2}{\partial K_1 \partial K_2} & \dots & 0 \\ \vdots & \vdots & \ddots & \vdots \\ 0 & 0 & \dots & \frac{\partial^2 \gamma_K}{\partial K_1 \partial K_2} \end{bmatrix}
 \end{aligned}$$

2.9 Implementation of the Estimation

The parameter estimation is implemented as described in section 2.5 and for comparison also by the solver-function of Matlab. For the weighted least square estimation, the inverse or, as can be seen from equation (65), the pseudo inverse of the sensitivity matrix \mathbf{S} is needed. For \mathbf{A} is a $n \times m$ ($n > m$) the pseudo inverse is:

$$\mathbf{A}^+ = (\mathbf{A}^\top \mathbf{A})^{-1} \mathbf{A}^\top \quad (116)$$

and has the main properties

$$\mathbf{A} \mathbf{A}^+ \mathbf{A} = \mathbf{A} \quad \mathbf{A}^+ \mathbf{A} \mathbf{A}^+ = \mathbf{A}^+ \quad (117)$$

If nevertheless $(\mathbf{A}^\top \mathbf{A})$ is ill conditioned, the truncated singular value decomposition *TSVD* is applied as regularization [2]. The singular value decomposition is a matrix factorization where

$$\mathbf{A} = \mathbf{U} \mathbf{\Sigma} \mathbf{V}^\top \quad (118)$$

- \mathbf{U} ... left singular vectors forming an unitary matrix
- $\mathbf{\Sigma}$... augmented diagonal matrix of singular values
- \mathbf{V} ... right singular vectors forming an unitary matrix

The matrix $\mathbf{\Sigma}$ has the same dimension as \mathbf{A} and is a diagonal matrix with positive descending singular values augmented by a zero matrix of the dimension $(n-m) \times m$. The

pseudo inverse \mathbf{A}^+ can be written as:

$$\begin{aligned}
\mathbf{A}^+ &= (\mathbf{A}^\top \mathbf{A})^{-1} \mathbf{A}^\top \\
\mathbf{A}^+ &= (\mathbf{V} \boldsymbol{\Sigma}^\top \mathbf{U}^\top \mathbf{U} \boldsymbol{\Sigma} \mathbf{V}^\top)^{-1} \mathbf{V} \boldsymbol{\Sigma}^\top \mathbf{U}^\top \\
\mathbf{A}^+ &= \mathbf{V} (\boldsymbol{\Sigma}^\top \boldsymbol{\Sigma})^{-1} \mathbf{V}^\top \mathbf{V} \boldsymbol{\Sigma}^\top \mathbf{U}^\top \\
\mathbf{A}^+ &= \mathbf{V} (\boldsymbol{\Sigma}^\top \boldsymbol{\Sigma})^{-1} \boldsymbol{\Sigma}^\top \mathbf{U}^\top \\
\mathbf{A}^+ &= \mathbf{V} \boldsymbol{\Sigma}^+ \mathbf{U}^\top
\end{aligned} \tag{119}$$

$\boldsymbol{\Sigma}^+$ is the pseudo inverse of $\boldsymbol{\Sigma}$ and is performed by transposing $\boldsymbol{\Sigma}$ and substituting the non-zero diagonal elements with their reciprocal values. The estimator is rewritten:

$$\begin{aligned}
\Delta \mathbf{p} &= (\mathbf{S}^\top \mathbf{W} \mathbf{S})^{-1} \mathbf{S}^\top \mathbf{W} [\mathbf{FRAP} - \mathbf{Frap}(\mathbf{p})] \\
\tilde{\mathbf{S}} &= \mathbf{Q} \mathbf{S} \quad \mathbf{Q} = \sqrt{\mathbf{W}}
\end{aligned} \tag{120}$$

$$\Delta \mathbf{p} = \tilde{\mathbf{S}}^+ \mathbf{Q} [\mathbf{FRAP} - \mathbf{Frap}(\mathbf{p})] \tag{121}$$

The elements of the diagonal matrix \mathbf{Q} are σ_i^{-1} , and so \mathbf{Q} is the square root of the weights of the WLS and equals the positive square root of the reciprocal variance of the data $\sqrt{\frac{1}{\sigma_i^2}}$. The singular value decomposition is used to regularize the ill conditioned $\tilde{\mathbf{S}}$ matrix by setting its too small singular values to zero before determining the pseudo inverse and the estimation step. This is the truncated singular value decomposition [3].

$$\tilde{\mathbf{S}} = \mathbf{U} \boldsymbol{\Sigma} \mathbf{V}^\top \tag{122}$$

$$\Delta \mathbf{p} = \mathbf{V} \tilde{\boldsymbol{\Sigma}}^+ \mathbf{U}^\top \mathbf{Q} [\mathbf{FRAP} - \mathbf{Frap}(\mathbf{p})] \tag{123}$$

Where $\tilde{\boldsymbol{\Sigma}}^+$ is pseudo inverse after regularization performed as described above. The chosen regularization criterion is: ‘‘If the singular value is smaller than 1% of the sum of singular values, than regularize it’’. This criterion takes into account the ratio of impact of each singular value on the estimation step. Very low singular values are produced through the limited accuracy of the numeric implementation.

For comparison of the implemented WLS estimator the built-in Matlab solver is used. The Matlab solver can be used to estimate the parameters with an objective function which gives the mean square error [MSE] to the measured data as a function of the parameters. Optionally the Jacobian and the Hessian of this objective function can be used to support the Matlab-solver. Therefore the mean square error and its Jacobian and Hessian have

to be defined

$$err = \frac{1}{N_T} [\mathbf{Frap}(\mathbf{p}) - \mathbf{FRAP}]^T \mathbf{W} [\mathbf{Frap}(\mathbf{p}) - \mathbf{FRAP}]$$

$$\mathbf{Jerr} = \frac{2}{N_T} \mathbf{S}^T \mathbf{W} [\mathbf{Frap}(\mathbf{p}) - \mathbf{FRAP}]$$

The Hessian of the mean square error:

$$\mathbf{Herr} = \begin{bmatrix} \frac{\partial^2 err}{\partial K_1^2} & \frac{\partial^2 err}{\partial K_1 \partial K_2} & \frac{\partial^2 err}{\partial K_1 \partial D} \\ \frac{\partial^2 err}{\partial K_1 \partial K_2} & \frac{\partial^2 err}{\partial K_2^2} & \frac{\partial^2 err}{\partial K_2 \partial D} \\ \frac{\partial^2 err}{\partial K_1 \partial D} & \frac{\partial^2 err}{\partial K_2 \partial D} & \frac{\partial^2 err}{\partial D^2} \end{bmatrix} \quad (124)$$

$$= \begin{bmatrix} \frac{\partial \mathbf{Jerr}}{\partial K_1} & \frac{\partial \mathbf{Jerr}}{\partial K_2} & \frac{\partial \mathbf{Jerr}}{\partial D} \end{bmatrix} \quad (125)$$

For one element one may write:

$$\frac{\partial \mathbf{Jerr}}{\partial K_1} = \frac{2}{N_T} \left(\begin{bmatrix} \frac{\partial^2 \mathbf{Frap}^T}{\partial K_1^2} \\ \frac{\partial^2 \mathbf{Frap}^T}{\partial K_1 \partial K_2} \\ \frac{\partial^2 \mathbf{Frap}^T}{\partial K_1 \partial D} \end{bmatrix} \mathbf{W} [\mathbf{Frap}(\mathbf{p}) - \mathbf{FRAP}] + \mathbf{S}^T \mathbf{W} \left[\frac{\partial \mathbf{Frap}}{\partial K_1} \right] \right)$$

$$= \frac{2}{N_T} \left((\mathbf{rH}_{[1-3]})^T \mathbf{W} [\mathbf{Frap}(\mathbf{p}) - \mathbf{FRAP}] + \mathbf{S}^T \mathbf{W} \mathbf{S}_{[1]} \right) \quad (126)$$

$\mathbf{rH}_{[1-3]}$... first to third column element of matrix \mathbf{rH} from equation (67)

$\mathbf{S}_{[1]}$... first column element of matrix \mathbf{S} from equation (66)

The calculation of \mathbf{Herr} is split into two parts, since both parts can be performed by one simple matrix multiplication. The first part is determined by $\mathbf{rH}^T \mathbf{W} [\mathbf{Frap}(\mathbf{p}) - \mathbf{FRAP}]$ and has to be rearranged to Hessian size. The second part is calculated by $\mathbf{S}^T \mathbf{W} \mathbf{S}$. The sum of both parts multiplied by $\frac{2}{N_T}$ is \mathbf{Herr} . The implementation of this construct is done by the following Matlab code:

```
%first part of differentiation of Gerr
%sum of residuals multiplied by elements of rearranged Hessian
A0=(Frap(:)-Frapm(:))'*W*Hessian;
%reshape to sum of Hessians in Hessian dimension
A1=reshape(A0,3,3);
%second part of differentiation of Gerr
A2=Jacobian'*W*Jacobian;
%hessian of error
Herr=(2/NT)*(A1+A2);
```


2.9.1 Covariance Matrix

To find the reliability of the parameter identification results, one may observe the covariance matrix [2].

$$\mathbf{CV} = (\mathbf{S}^T \mathbf{W} \mathbf{S})^{-1} \quad (127)$$

To provide the covariance of the weighted least square estimator the variances of the data have to be known. The weights of the estimation are the reciprocal values of the data variances. Assuming constant data variance, \mathbf{CV} can be interpreted as scaling factors of data variance.

2.10 Spatial FRAP Model

As the FRAP data are derived from measurements of spatial distributed pixels, the spatial information assists the estimation in becoming more stable or accurate. Therefore the model has to be redesigned to predict the spatial FRAP data. The chosen approaches are

- disks
- rings

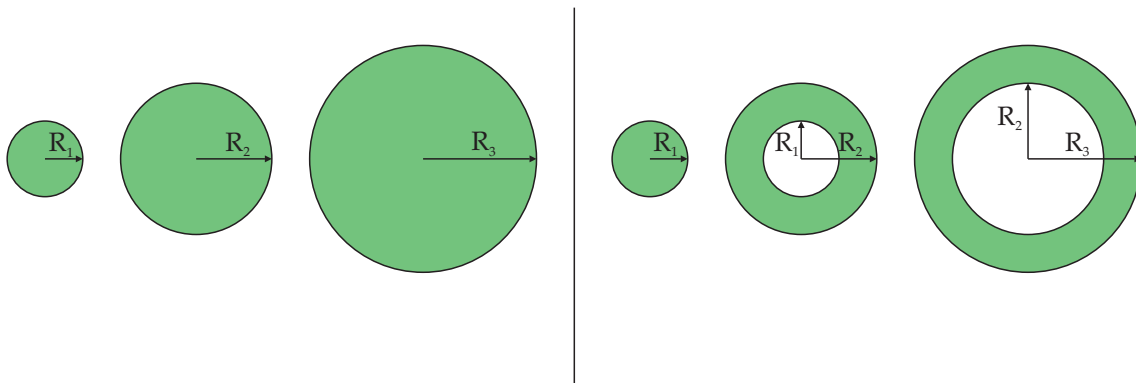


Figure 3: two approaches for spatial Frap, shown for one timestamp: left Disks, right Rings

The variance of disk FRAP-data is spatial descending through the ascending averaging area. Whereas the ring Frap-data represent with each ring “new, unused” information for the estimation model, and the rings are independent to each other.

As each disk is a single FRAP measurement the extended model with N_R disks can be

presented:

$$\text{Frap}(t) = \frac{2\pi}{\pi R^2} \int_0^R r \text{frap}(r, t) dr \quad (128)$$

$$\text{Frap}_n = \frac{2}{R_n^2} \int_0^{R_n} r \text{frap}(r, t) dr \quad (129)$$

$$\mathbf{Frap}_n = [\text{Frap}_n(t_1) \quad \dots \quad \text{Frap}_n(t_{NT})]^\top \quad (130)$$

$$\mathbf{FrapDisk} = \begin{bmatrix} \mathbf{Frap}_1 \\ \vdots \\ \mathbf{Frap}_{NR} \end{bmatrix} \quad (131)$$

$$\mathbf{SDisk} = \begin{bmatrix} \mathbf{S}_1 \\ \vdots \\ \mathbf{S}_{NR} \end{bmatrix} \quad (132)$$

$$\mathbf{rHDisk} = \begin{bmatrix} \mathbf{rH}_1 \\ \vdots \\ \mathbf{rH}_{NR} \end{bmatrix} \quad (133)$$

$$\mathbf{WDisk} = \begin{bmatrix} \mathbf{W}_1 & \dots & 0 \\ \vdots & \ddots & \vdots \\ 0 & \dots & \mathbf{W}_{NR} \end{bmatrix} \quad (134)$$

The ring FRAP model has to be derived from the FRAP model.

$$\text{Frap}_n = \frac{2}{R_n^2} \int_0^{R_n} r \text{frap}(r, t) dr = \frac{2}{R_n^2} \left[\int_0^{R_{n-1}} r \text{frap}(r, t) dr + \int_{R_{n-1}}^{R_n} r \text{frap}(r, t) dr \right]$$

$$\frac{R_n^2}{2} \text{Frap}_n = \frac{R_{n-1}^2}{2} \text{Frap}_{n-1}(t) + \int_{R_{n-1}}^{R_n} r \text{frap}(r, t) dr$$

$$\frac{A_{\text{Ring}_n}}{2\pi} \text{FrapRing}_n(t) = \frac{R_n^2}{2} \text{Frap}_n(t) - \frac{R_{n-1}^2}{2} \text{Frap}_{n-1}(t)$$

$$\boxed{\text{FrapRing}_n(t) = \frac{R_n^2 \text{Frap}_n(t) - R_{n-1}^2 \text{Frap}_{n-1}(t)}{R_n^2 - R_{n-1}^2}} \quad (135)$$

$$\mathbf{FrapRing}_n = [\text{FrapRing}_n(t_1) \quad \dots \quad \text{FrapRing}_n(t_{NT})]^\top$$

The Jacobian \mathbf{SRing}_n and rearranged matrix \mathbf{rHRing}_n of $\mathbf{FrapRing}_n$ are constructed analogously

$$\mathbf{SRing}_n = \left[\frac{\partial \mathbf{FrapRing}_n}{\partial K_1} \quad \frac{\partial \mathbf{FrapRing}_n}{\partial K_2} \quad \frac{\partial \mathbf{FrapRing}_n}{\partial D} \right] \quad (136)$$

$$\frac{\partial \mathbf{FrapRing}_n}{\partial K_1} = \frac{R_n^2}{R_n^2 - R_{n-1}^2} \frac{\partial \mathbf{Frap}_n}{\partial K_1} - \frac{R_{n-1}^2}{R_n^2 - R_{n-1}^2} \frac{\partial \mathbf{Frap}_{n-1}}{\partial K_1} \quad (137)$$

The differentiation with respect to K_2 or D is done in a similar way.

$$\begin{aligned} \mathbf{rHRing}_n &= \left[\frac{\partial \mathbf{SRing}_n}{\partial K_1} \quad \frac{\partial \mathbf{SRing}_n}{\partial K_2} \quad \frac{\partial \mathbf{SRing}_n}{\partial D} \right] \\ &= \left[\frac{\partial^2 \mathbf{FrapRing}_n}{\partial K_1^2} \quad \frac{\partial^2 \mathbf{FrapRing}_n}{\partial K_1 \partial K_2} \quad \frac{\partial^2 \mathbf{FrapRing}_n}{\partial K_1 \partial D} \quad \dots \right. \\ &\quad \frac{\partial^2 \mathbf{FrapRing}_n}{\partial K_2 \partial K_1} \quad \frac{\partial^2 \mathbf{FrapRing}_n}{\partial K_2^2} \quad \frac{\partial^2 \mathbf{FrapRing}_n}{\partial K_2 \partial D} \quad \dots \\ &\quad \left. \frac{\partial^2 \mathbf{FrapRing}_n}{\partial D \partial K_1} \quad \frac{\partial^2 \mathbf{FrapRing}_n}{\partial D \partial K_2} \quad \frac{\partial^2 \mathbf{FrapRing}_n}{\partial D^2} \right] \quad (138) \end{aligned}$$

$$\frac{\partial^2 \mathbf{FrapRing}_n}{\partial K_1 \partial K_2} = \frac{R_n^2}{R_n^2 - R_{n-1}^2} \frac{\partial^2 \mathbf{Frap}_n}{\partial K_1 \partial K_2} - \frac{R_{n-1}^2}{R_n^2 - R_{n-1}^2} \frac{\partial^2 \mathbf{Frap}_{n-1}}{\partial K_1 \partial K_2} \quad (139)$$

All second derivations in respect to K_1 , K_2 and D are done in a similar way. The complete set of functions for parameter estimation is presented:

$$\mathbf{FrapRing} = \begin{bmatrix} \mathbf{Frap}_1 \\ \mathbf{FrapRing}_2 \\ \vdots \\ \mathbf{FrapRing}_{NR} \end{bmatrix} \quad (140)$$

$$\mathbf{SRing} = \begin{bmatrix} \mathbf{S}_1 \\ \mathbf{SRing}_2 \\ \vdots \\ \mathbf{SRing}_{NR} \end{bmatrix} \quad (141)$$

$$\mathbf{rHRing} = \begin{bmatrix} \mathbf{rH}_1 \\ \mathbf{rHRing}_2 \\ \vdots \\ \mathbf{rHRing}_{NR} \end{bmatrix} \quad (142)$$

$$\mathbf{WRing} = \begin{bmatrix} \mathbf{W}_1 & \dots & 0 \\ \vdots & \ddots & \vdots \\ 0 & \dots & \mathbf{W}_{NR} \end{bmatrix} \quad (143)$$

The disk FRAP model and the ring FRAP model can be performed with the implemented derivations of the FRAP model as is shown in equations (135),(137) and (139). After these calculations the estimation is proceeded similarly as in section 2.9, with regard to the changed $\tilde{N}_T = N_T N_R$. For completeness the needed formulas are pictures again.

$$\begin{aligned}\Delta \mathbf{p} &= (\mathbf{S}^T \mathbf{W} \mathbf{S})^{-1} \mathbf{S}^T \mathbf{W} [\mathbf{FRAP} - \mathbf{Frap}(\mathbf{p})] \\ err &= \frac{1}{N_T} [\mathbf{Frap}(\mathbf{p}) - \mathbf{FRAP}]^T \mathbf{W} [\mathbf{Frap}(\mathbf{p}) - \mathbf{FRAP}] \\ \mathbf{Jerr} &= \frac{2}{N_T} \mathbf{S}^T \mathbf{W} [\mathbf{Frap}(\mathbf{p}) - \mathbf{FRAP}] \\ \mathbf{Herr} &= \begin{bmatrix} \frac{\partial \mathbf{Jerr}}{\partial K_1} & \frac{\partial \mathbf{Jerr}}{\partial K_2} & \frac{\partial \mathbf{Jerr}}{\partial D} \end{bmatrix} \\ \frac{\partial \mathbf{Jerr}}{\partial K_1} &= \frac{2}{N_T} \left((\mathbf{rH}_{[1-3]})^T \mathbf{W} [\mathbf{Frap}(\mathbf{p}) - \mathbf{FRAP}] + \mathbf{S}^T \mathbf{W} \mathbf{S}_{[1]} \right)\end{aligned}$$

For the disk and ring FRAP model the corresponding matrices have to be used, ***FrapDisk***, ***SDisk***, ***rHDisk***, ***WDisk***, ***FRAPDisk*** for the disk FRAP model and ***FrapRing***, ***SRing***, ***rHRing***, ***WRing***, ***FRAPRing*** for the ring FRAP model.

3 Results

The presented results are produced by the implemented estimation methods. These estimators are referred to as

- WLS: weighted least square estimation
- error-solver: solver-function of Matlab, objective function is the mean square error
- gradient-solver: solver function of Matlab, objective function is the mean square error, with user defined gradient function of mean square error
- hessian-solver: solver function of Matlab, objective function is the mean square error, with user defined Hessian function of mean square error

3.1 Determining K_b

The bleaching due to imaging rate K_b has to be known exactly. An simultaneous identification with the reaction rates cannot be established. Therefore great effort was set in identifying K_b from the data at hand. In the FRAP model K_b appears as an exponential decay function. An identification method is established to find the best identification for K_b from the unbleached and the pre-bleached present data. An inverse problem is defined, where the forward problem is an logarithmic calculus system describing the decay rate of each pixel. Negative values, as can occur in the preprocessing of the data, have to be redefined for the logarithmical problem. To solve the inverse problem the analytical Jacobian and Hessian for each pixel are determined and with these the estimation of the parameter K_b performed. The complex calculations lead for the different regions to different rates, these differences are in a minor order of magnitude. The results are averaged in order to find a good estimation of the effective K_b .

3.2 Estimation of K_1 and K_2

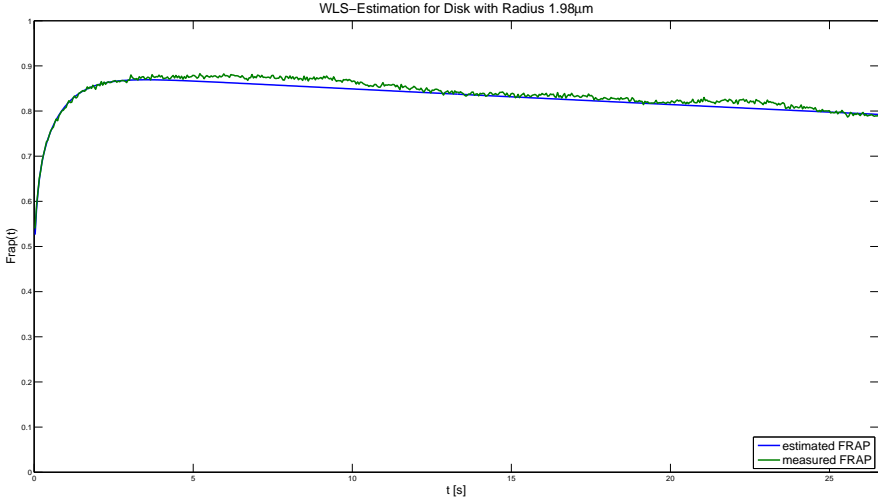


Figure 4: Estimated FRAP and measured FRAP

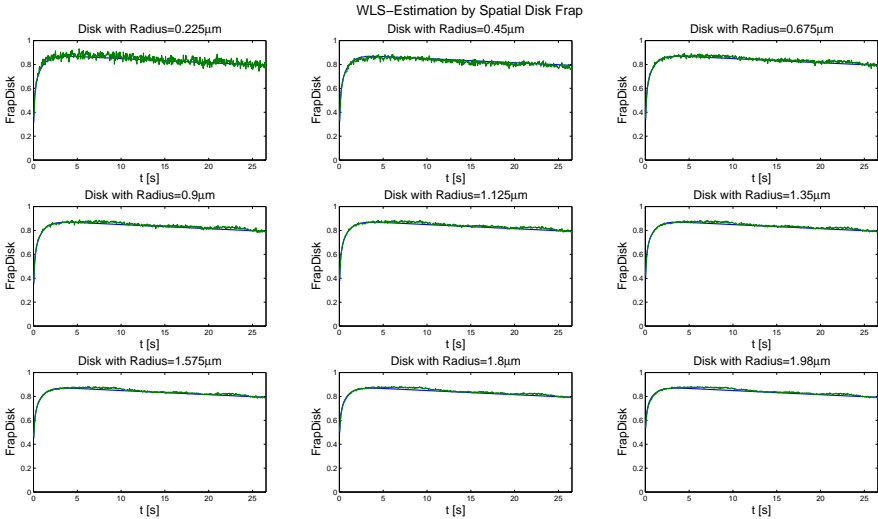


Figure 5: Disk Model: estimated FRAP and measured FRAP

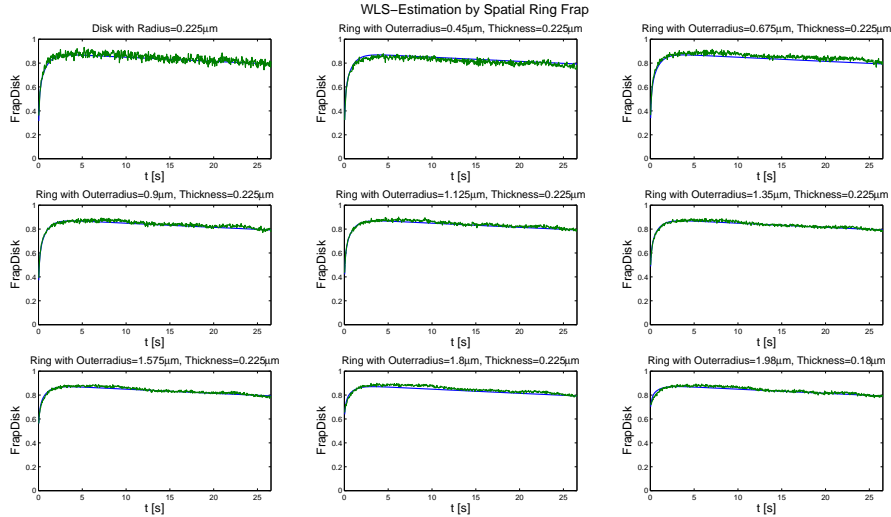


Figure 6: Ring Model: estimated FRAP and measured FRAP

3.2.1 Effect of the Number of Terms of Bessel Series

Effect on Approximating the Initials Distribution

For the shown FRAP-Model the initial distribution has to be approximated with an Bessel series expansion. The number of Bessel terms used for this expansion have the following effects on the estimation. As absolute runtime values depend on the processing machine but relative runtime values don't, the presented time values are normalized to the smallest corresponding runtime. The mean square error [MSE] of the approximation to the assumed gaussian decay and the MSE to the Bessel series expansion with 50 Terms are presented for comparison.(see table 2).

Terms	Time Consumption	MSE to Gaussian Decay	MSE to 50 Terms-Expansion
50	1	4.1649e-5	
100	2.51	4.1652e-5	6.8840e-10
200	5.78	4.1652e-5	6.8710e-10
500	13.91	4.1652e-5	6.9104e-10

Table 2: Number of Bessel Terms and its Effect on the Approximation of the Initial Distribution

Effect on Estimation

Table 3 presents the normalized runtime [t_{est}], the number of iteration steps [it.] and the estimation MSE of the four implemented estimation methods for different numbers of terms of the Bessel series expansion used in the FRAP-model.

Method	Terms	t_{est}	it.	Estimation MSE
WLS	50	1	8	0.1072e-3
	100	1.17	8	0.1072e-3
	200	1.82	8	0.1072e-3
	500	3.33	8	0.1072e-3
error-solver	50	1	19	0.1072e-3
	100	1.05	19	0.1072e-3
	200	1.30	19	0.1072e-3
	500	1.73	19	0.1072e-3
gradient-solver	50	1	5	0.1072e-3
	100	1.15	5	0.1072e-3
	200	1.62	5	0.1072e-3
	500	2.82	5	0.1072e-3
Hessian-solver	50	1	5	0.1072e-3
	100	1.24	5	0.1072e-3
	200	1.89	5	0.1072e-3
	500	3.78	5	0.1072e-3

Table 3: Number of Bessel terms and its Effect on Estimating K_1, K_2

Method	Terms	t_{est}	it.	Estimation MSE
disk-WLS	50	1	6	0.1839e-3
	100	1.35	6	0.1839e-3
	200	2.23	6	0.1839e-3
	500	5.16	6	0.1839e-3
disk-error-solver	50	1	18	0.1839e-3
	100	1.53	18	0.1839e-3
	200	2.68	18	0.1839e-3
	500	5.34	18	0.1839e-3
disk-gradient-solver	50	1	4	0.1839e-3
	100	1.56	4	0.1839e-3
	200	3.18	4	0.1839e-3
	500	6.86	4	0.1839e-3
disk-Hessian-solver	50	1	4	0.1839e-3
	100	1.72	4	0.1839e-3
	200	3.63	4	0.1839e-3
	500	9.28	4	0.1839e-3

Table 4: Number of Bessel terms and its Effect on Estimating K_1, K_2 by Disk Model

Method	Terms	t_{est}	it.	Estimation MSE
ring-WLS	50	1	8	0.2970e-3
	100	1.39	8	0.2970e-3
	200	2.32	8	0.2970e-3
	500	5.67	8	0.2970e-3
ring-error-solver	50	1	18	0.2970e-3
	100	1.49	18	0.2970e-3
	200	2.67	18	0.2970e-3
	500	5.22	18	0.2970e-3
ring-gradient-solver	50	1	4	0.2970e-3
	100	1.57	4	0.2970e-3
	200	3.22	4	0.2970e-3
	500	7.47	4	0.2970e-3
ring-Hessian-solver	50	1	4	0.2970e-3
	100	1.70	4	0.2970e-3
	200	3.58	4	0.2970e-3
	500	8.25	4	0.2970e-3

Table 5: Number of Bessel terms and its Effect on Estimating K_1, K_2 by Ring Model

3.2.2 Sensitivity to the Choice of Start Parameters

The different estimation methods are tested for the robustness against the choice of the start parameters. Therefore, in the lack of known reaction rates, an expected result for K_1 and K_2 is generated by the estimators. Only the results in the same order of magnitude of the expected result $K_{1,exp}, K_{2,exp}$ are rated as successful.

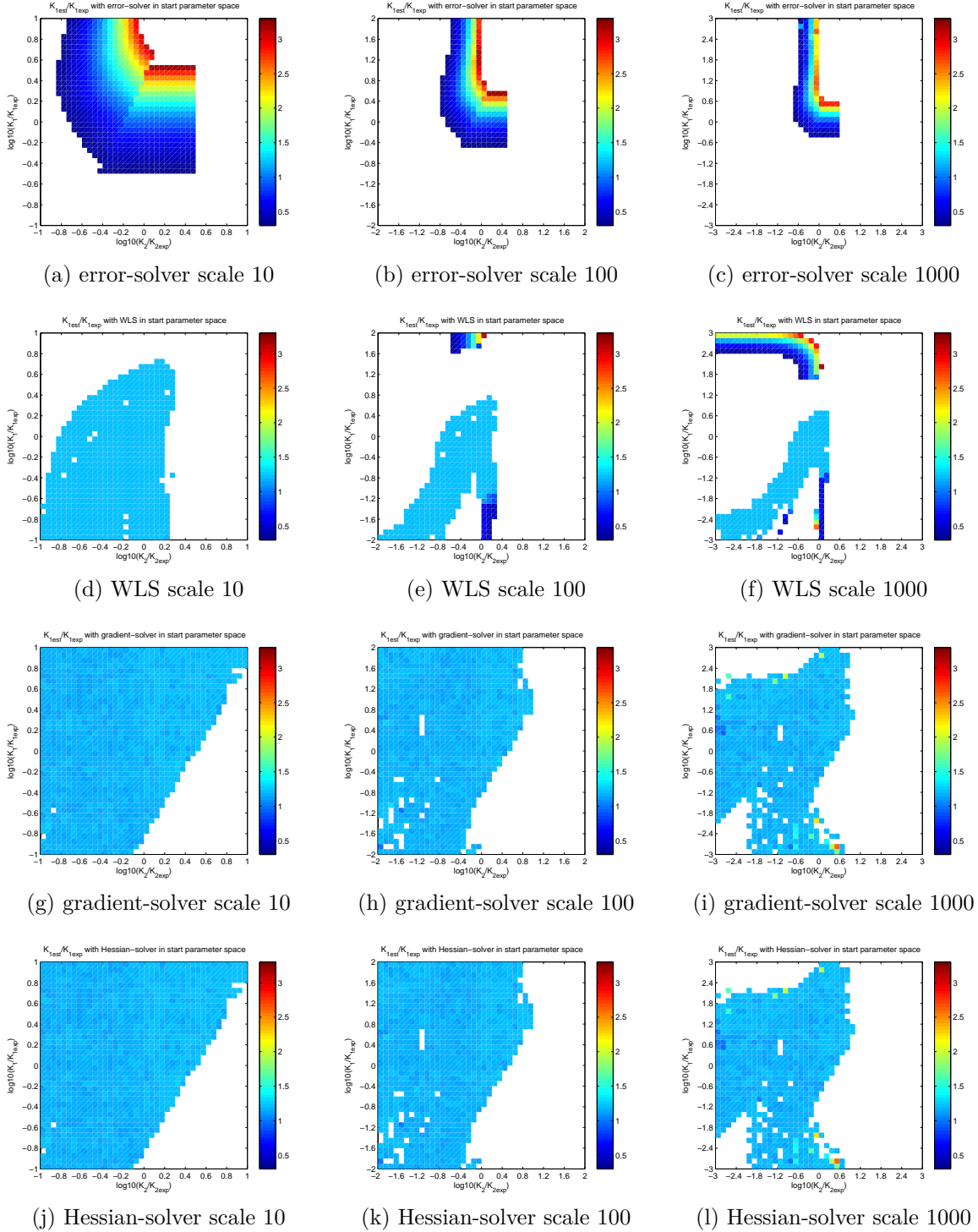
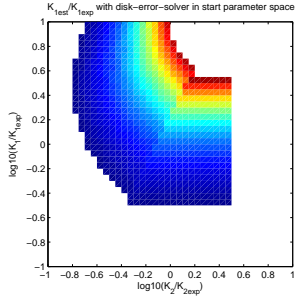
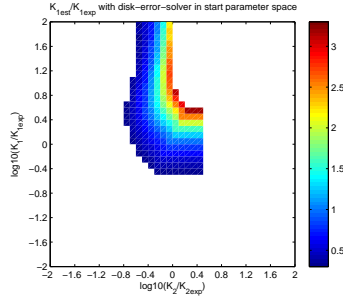


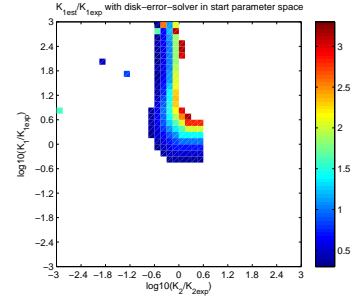
Figure 7: successful estimations of K_1 in start parameter space



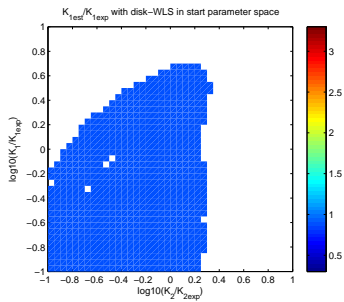
(a) disk-error-solver scale 10



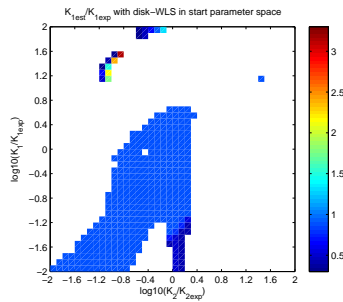
(b) disk-error-solver scale 100



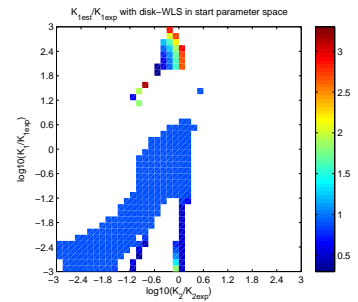
(c) disk-error-solver scale 1000



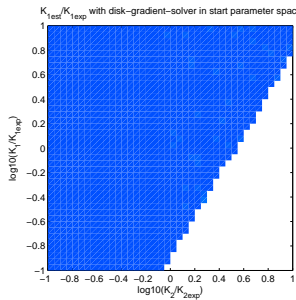
(d) disk-WLS scale 10



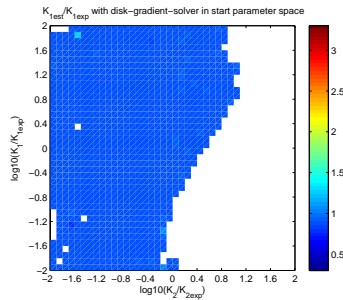
(e) disk-WLS scale 100



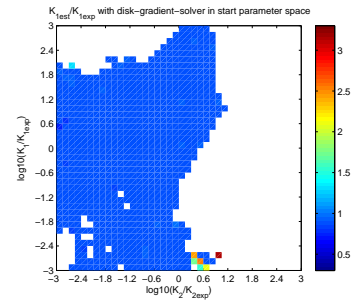
(f) disk-WLS scale 1000



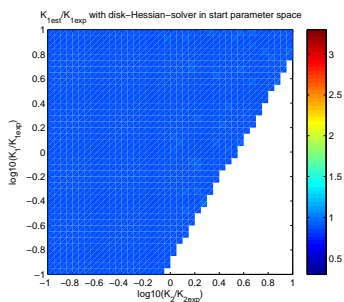
(g) disk-gradient-solver scale 10



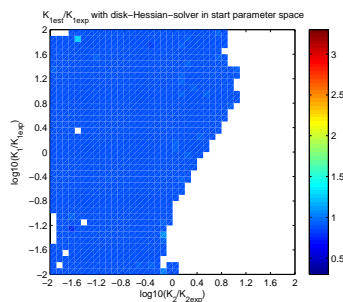
(h) disk-gradient-solver scale 100



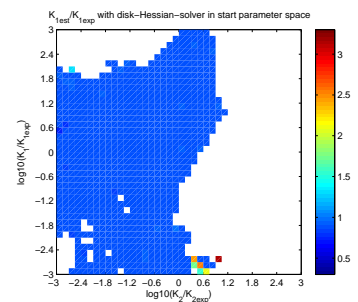
(i) disk-gradient-solver scale 1000



(j) disk-Hessian-solver scale 10

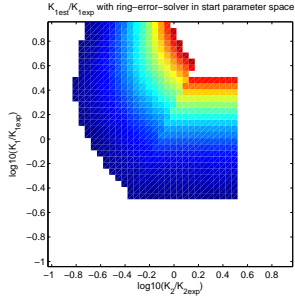


(k) disk-Hessian-solver scale 100

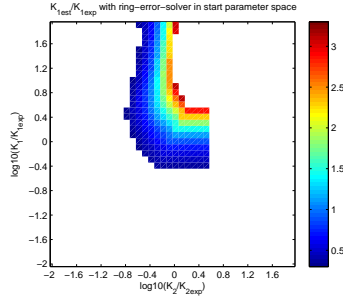


(l) disk-Hessian-solver scale 1000

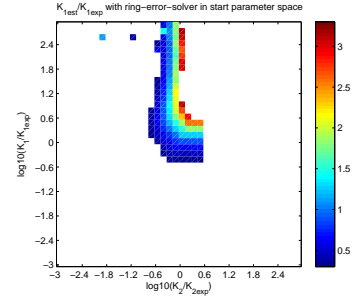
Figure 8: successful estimations of K_1 in start parameter space by disk model



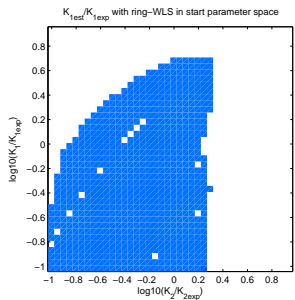
(a) ring-error-solver scale 10



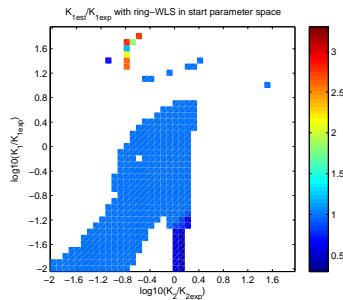
(b) ring-error-solver scale 100



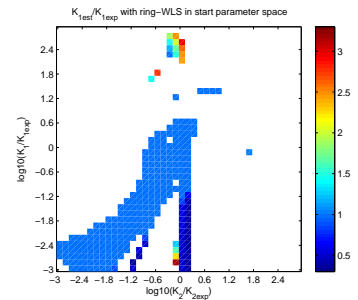
(c) ring-error-solver scale 1000



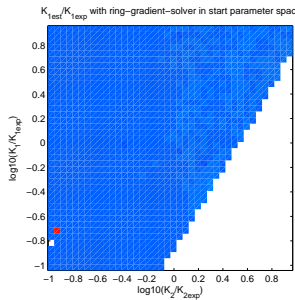
(d) ring-WLS scale 10



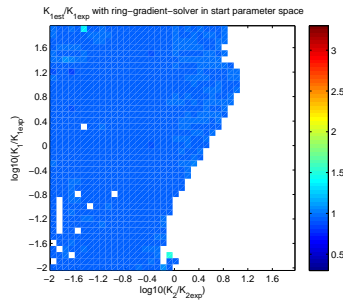
(e) ring-WLS scale 100



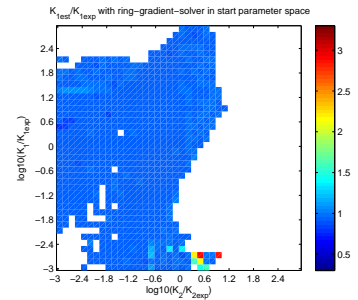
(f) ring-WLS scale 1000



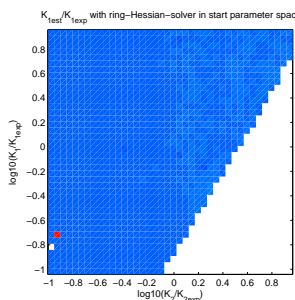
(g) ring-gradient-solver scale 10



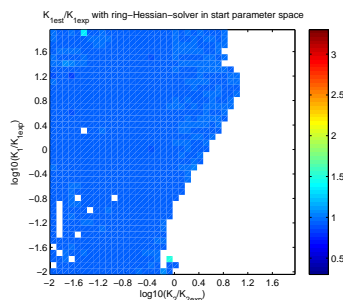
(h) ring-gradient-solver scale 100



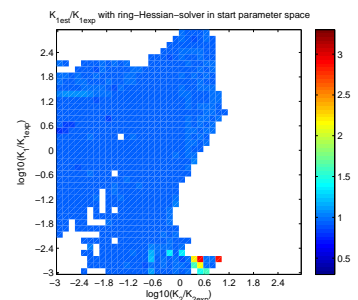
(i) ring-gradient-solver scale 1000



(j) ring-Hessian-solver scale 10



(k) ring-Hessian-solver scale 100



(l) ring-Hessian-solver scale 1000

Figure 9: successful estimations of K_1 in start parameter space by ring model

3.2.3 Comparison of Estimators

Terms	Method	t_{est}	it.	K1	K2	
50	WLS	1	8	0.8892	1.4484	
	error-solver	10.22	19	0.8892	1.4484	
	gradient-solver	4.03	5	0.8892	1.4484	
	Hessian-solver	2.36	5	0.8892	1.4484	
	disk-WLS	1.10	6	0.6494	1.3088	
	disk-error-solver	9.36	18	0.6493	1.3088	
	disk-gradient-solver	8.18	4	0.6494	1.3088	
	disk-Hessian-solver	5.93	4	0.6494	1.3088	
	ring-WLS	1.42	8	0.6909	1.3455	
	ring-error-solver	9.51	18	0.6909	1.3455	
	ring-gradient-solver	8.00	4	0.6909	1.3455	
	ring-Hessian-solver	6.02	4	0.6909	1.3455	
100	WLS	1.17				
	error-solver	10.69				
	gradient-solver	4.64				
	Hessian-solver	2.92				
	disk-WLS	1.48				
	disk-error-solver	14.33	identical results as with 50 Terms			
	disk-gradient-solver	12.73				
	disk-Hessian-solver	10.21				
	ring-WLS	1.98				
	ring-error-solver	14.14				
	ring-gradient-solver	12.54				
	ring-Hessian-solver	10.23				
500	WLS	3.33				
	error-solver	17.64				
	gradient-solver	11.36				
	Hessian-solver	8.93				
	disk-WLS	5.66				
	disk-error-solver	50.01	identical results as with 50 Terms			
	disk-gradient-solver	56.12				
	disk-Hessian-solver	54.99				
	ring-WLS	8.08				
	ring-error-solver	49.69				
	ring-gradient-solver	59.73				
	ring-Hessian-solver	49.68				

Table 6: Number of Bessel terms and its Effect on Estimating K_1, K_2 by Ring Model

3.2.4 Covariance of Weighted Least Square Estimator

The parameter identification using the weighted least square method leads to the results (table 7). The covariance matrix for the estimations is calculated by equation (127).

K1	K2
0.8166	1.3670

Table 7: estimated parameters with given variance

$$CV = \begin{bmatrix} 43.1563 & 25.0450 \\ 25.0450 & 16.0750 \end{bmatrix} \quad (144)$$

$$CV_{RING} = \begin{bmatrix} 31.4362 & 21.7458 \\ 21.7458 & 16.7976 \end{bmatrix} \quad (145)$$

$$CV_{DISK} = \begin{bmatrix} 4.9843 & 3.3593 \\ 3.3593 & 2.5278 \end{bmatrix} \quad (146)$$

3.3 Estimation of K_1 , K_2 and D

3.3.1 Effect of the Number of Terms of Bessel Series

Effect on Estimation

Table 3 presents the normalized runtime t_{est} and the estimation MSE of the four implemented estimation methods for different number of terms of the Bessel series expansion used in the FRAP-model. For the disk and ring Frap-model this is shown in tables 4, 5.

Method	Terms	t_{est}	it.	Estimation MSE
WLS	50	1	8	0.1061e-3
	100	1.28	8	0.1067e-3
	200	1.91	8	0.1067e-3
	500	3.79	8	0.1067e-3
error-solver	50	1	27	0.1061e-3
	100	1.16	27	0.1067e-3
	200	1.57	27	0.1067e-3
	500	2.59	27	0.1067e-3
gradient-solver	50	1	13	0.1061e-3
	100	1.62	13	0.1067e-3
	200	3.30	13	0.1067e-3
	500	7.78	13	0.1067e-3
Hessian-solver	50	1	13	0.1061e-3
	100	1.69	13	0.1067e-3
	200	2.93	13	0.1067e-3
	500	7.30	13	0.1067e-3

Table 8: Number of Bessel terms and its Effect on Estimating K_1, K_2 and D

Method	Terms	t_{est}	it.	Estimation MSE
disk-WLS	50	1	6	0.1839e-3
	100	1.40	6	0.1839e-3
	200	2.24	6	0.1839e-3
	500	4.95	6	0.1839e-3
disk-error-solver	50	1	31	0.1839e-3
	100	1.45	31	0.1839e-3
	200	2.42	31	0.1839e-3
	500	5.58	31	0.1839e-3
disk-gradient-solver	50	1	12	0.1839e-3
	100	1.70	12	0.1839e-3
	200	3.53	12	0.1839e-3
	500	8.86	12	0.1839e-3
disk-Hessian-solver	50	1	12	0.1839e-3
	100	7.33	12	0.1839e-3
	200	14.95	12	0.1839e-3
	500	35.44	12	0.1839e-3

Table 9: Number of Bessel terms and its Effect on Estimating K_1, K_2 and D by Disk Model

Method	Terms	t_{est}	it.	Estimation MSE
ring-WLS	50	1	max	0.2970e-3
	100	1.62	max	0.2970e-3
	200	3.12	max	0.2970e-3
	500	7.10	max	0.2970e-3
ring-error-solver	50	1	33	0.2970e-3
	100	1.45	33	0.2970e-3
	200	2.47	33	0.2970e-3
	500	5.88	33	0.2970e-3
ring-gradient-solver	50	1	41	0.2970e-3
	100	1.65	41	0.2970e-3
	200	3.37	41	0.2970e-3
	500	8.36	41	0.2970e-3
ring-Hessian-solver	50	1	41	0.2970e-3
	100	23.3	41	0.2970e-3
	200	47.47	41	0.2970e-3
	500	128.04	41	0.2970e-3

Table 10: Number of Bessel terms and its Effect on Estimating K_1, K_2 and D by Ring Model

3.3.2 Sensitivity to the Choice of Start Parameters

For the presentation of the estimators in the start parameter space, $K_{1,start}$ varies from $\frac{1}{sf}K_{1,exp}$ to $sfK_{1,exp}$ with sf as scaling factor and the same for $K_{2,start}$. The scaling factor of D_{start} is set to 5 and is shown in 9 subplots. Successful estimations are defined by the concurrent constraints for the results of K_1 and K_2 being in the same order of magnitude as the expected values and D being in the interval $\frac{1}{1.5}D_{exp} - 1.5D_{exp}$.

Estimation of K_1, K_2 and D

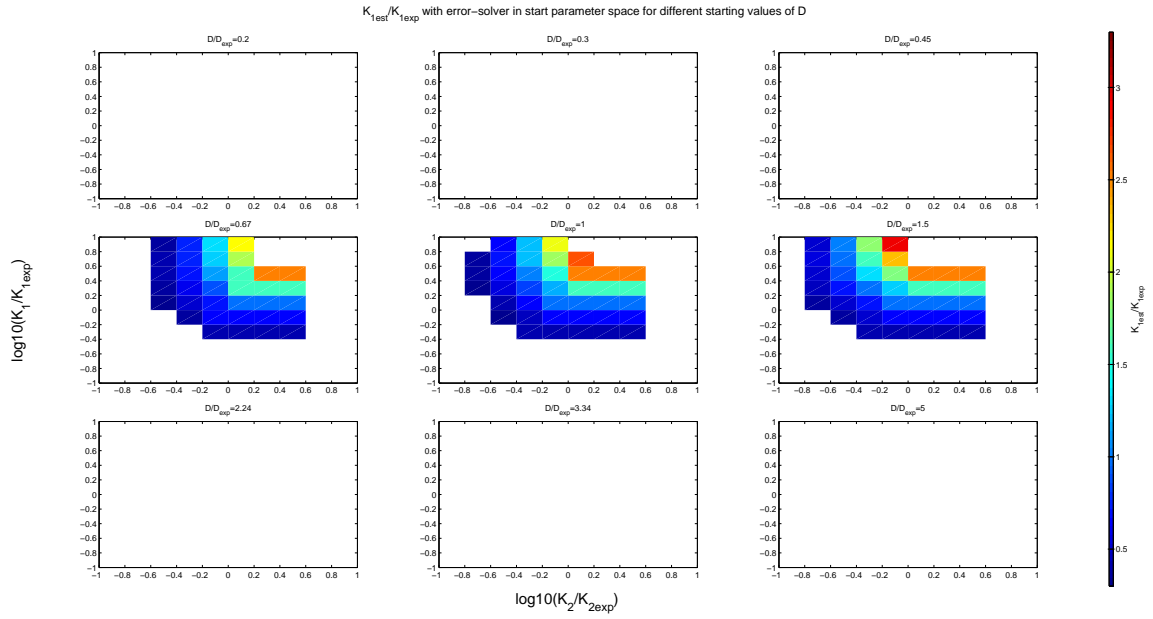


Figure 10: error-solver estimations of K_1 in start parameter space for different D_{start} scale 10

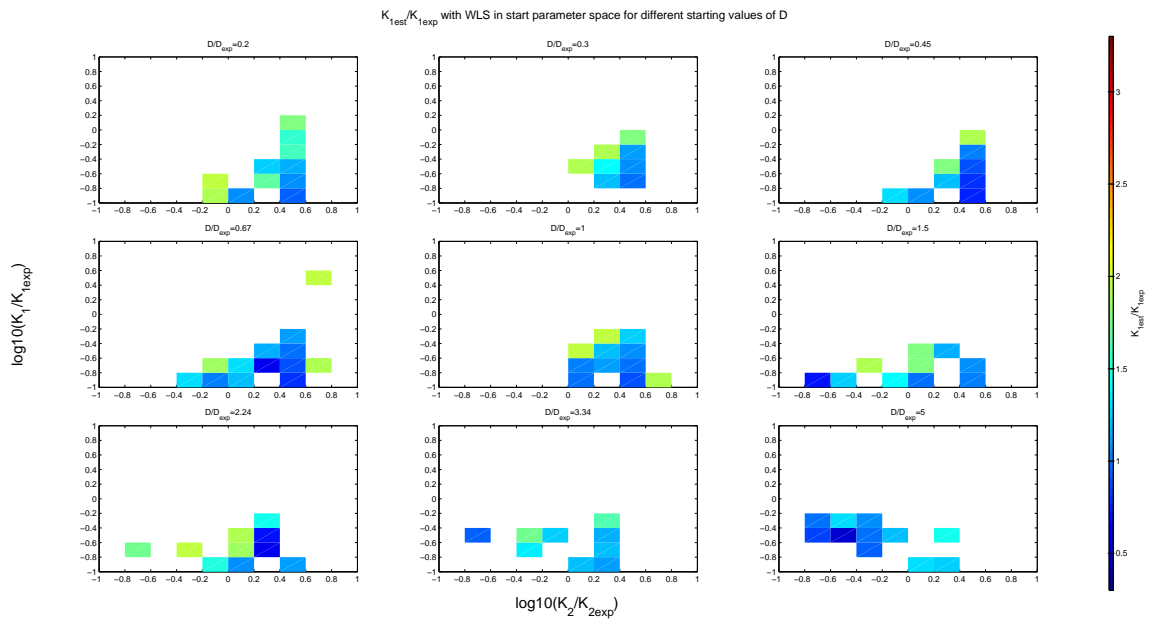


Figure 11: WLS estimations of K_1 in start parameter space for different D_{start} scale 10

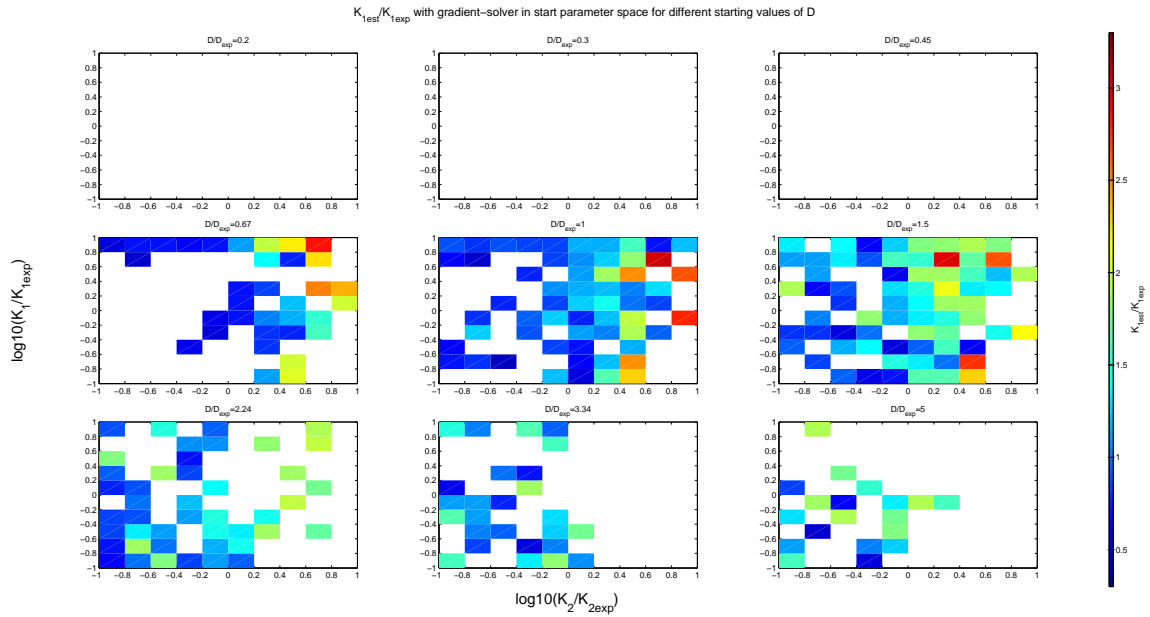


Figure 12: gradient-solver estimations of K_1 in start parameter space for different D_{start} scale 10

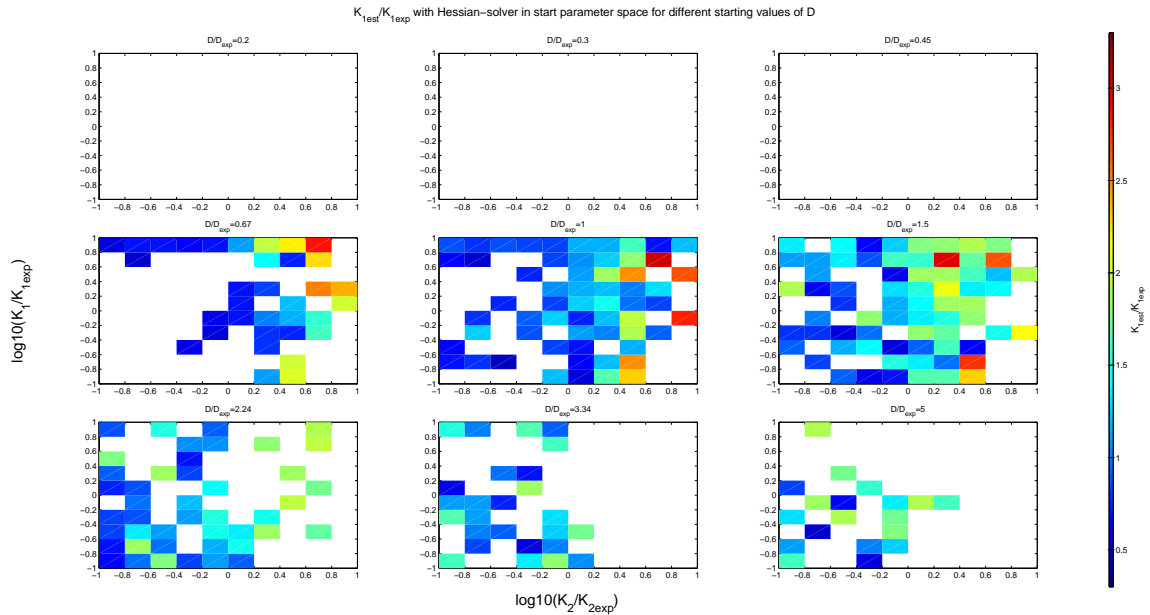


Figure 13: Hessian-solver estimations of K_1 in start parameter space for different D_{start} scale 10

Estimation of K_1, K_2 and D by Disk-Model

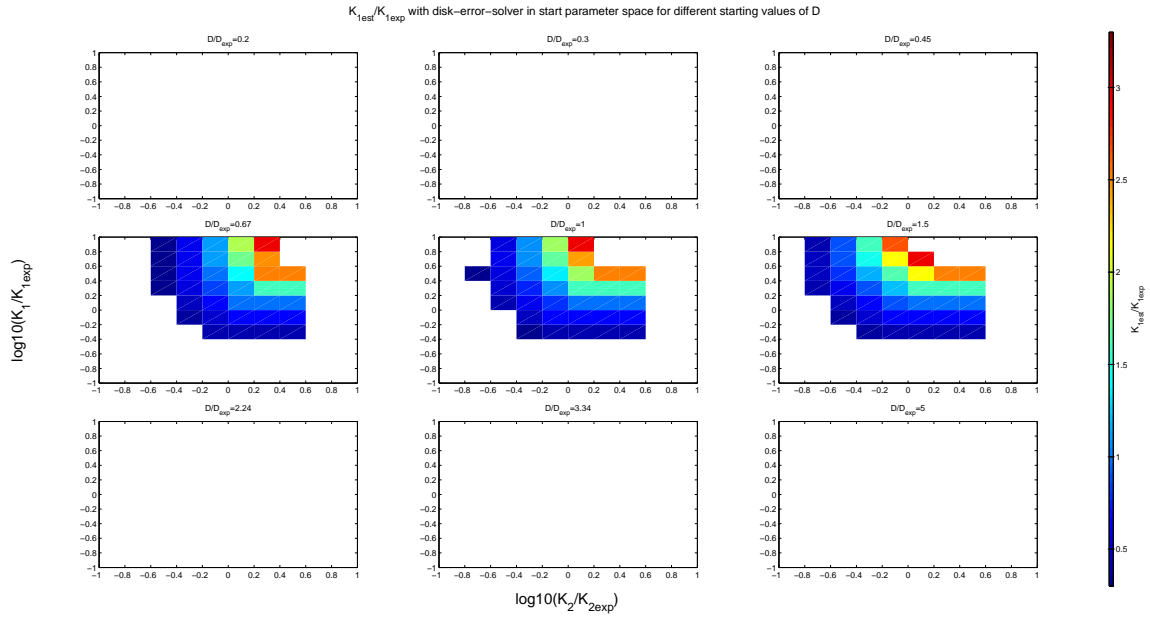


Figure 14: error-solver estimations of K_1 in start parameter space for different D_{start} scale 10

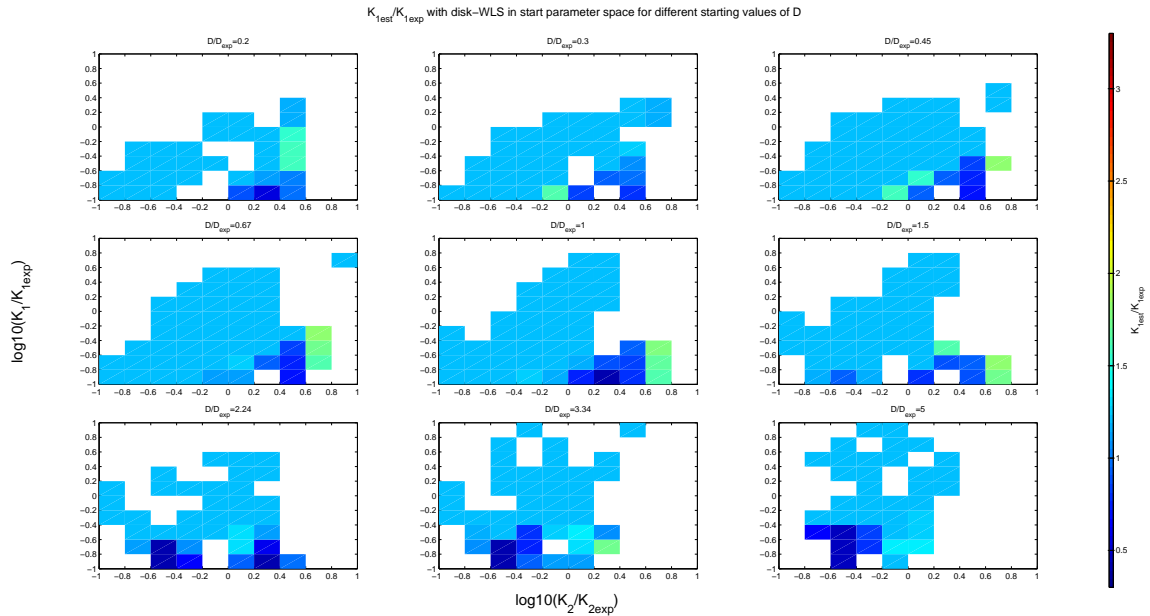


Figure 15: WLS estimations of K_1 in start parameter space for different D_{start} scale 10

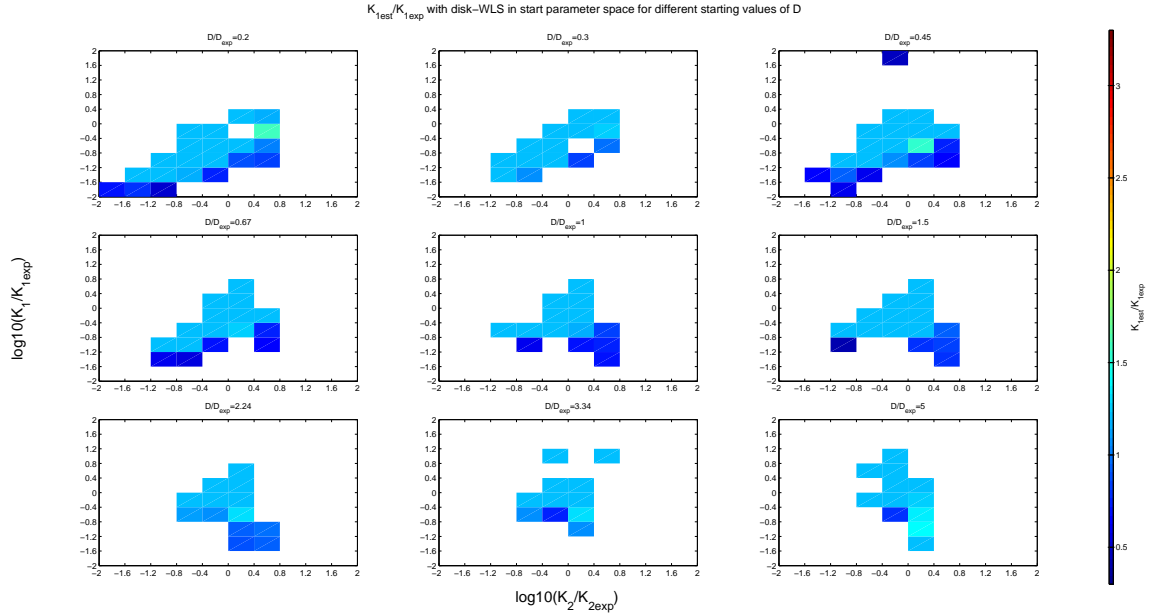


Figure 16: WLS estimations of K_1 in start parameter space for different D_{start} scale 100

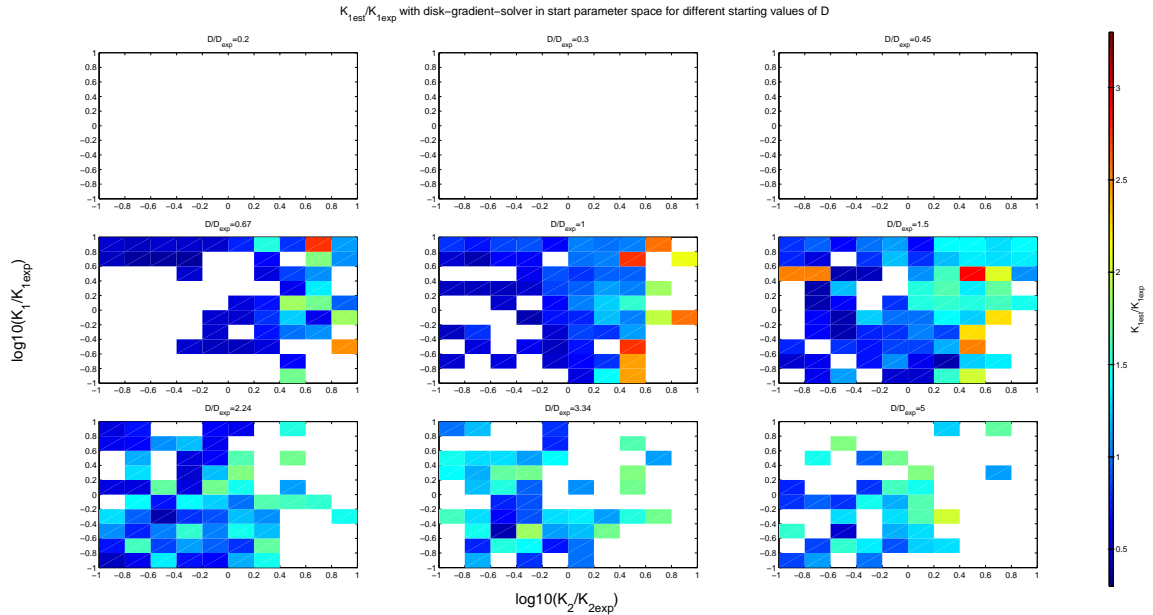


Figure 17: gradient-solver estimations of K_1 in start parameter space for different D_{start} scale 10

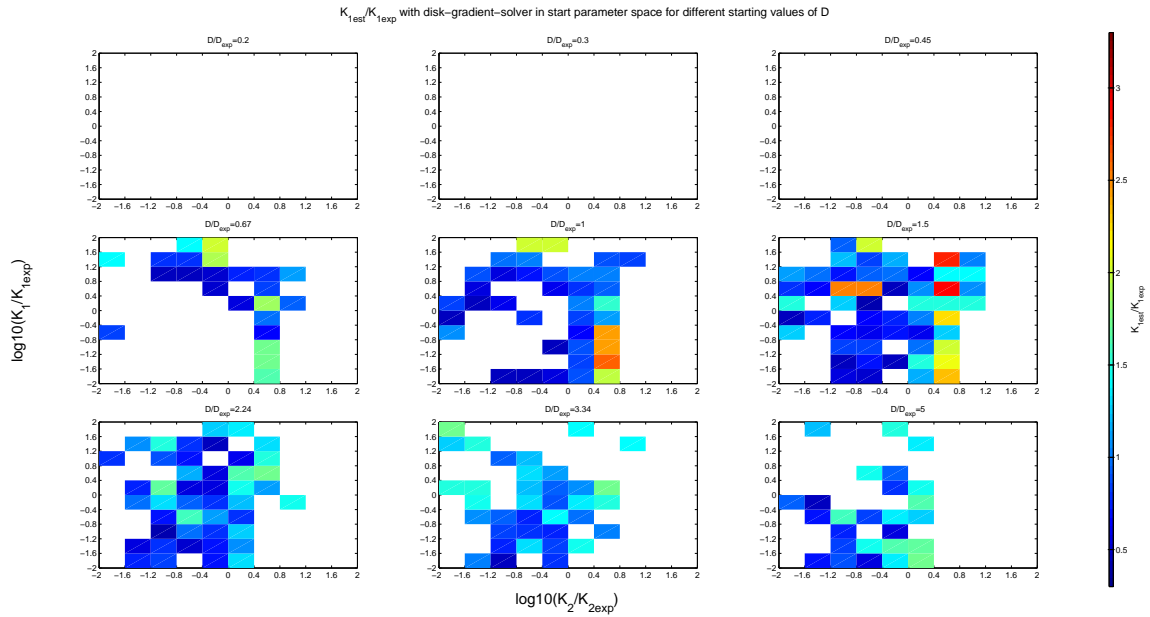


Figure 18: gradient-solver estimations of K_1 in start parameter space for different D_{start} scale 100

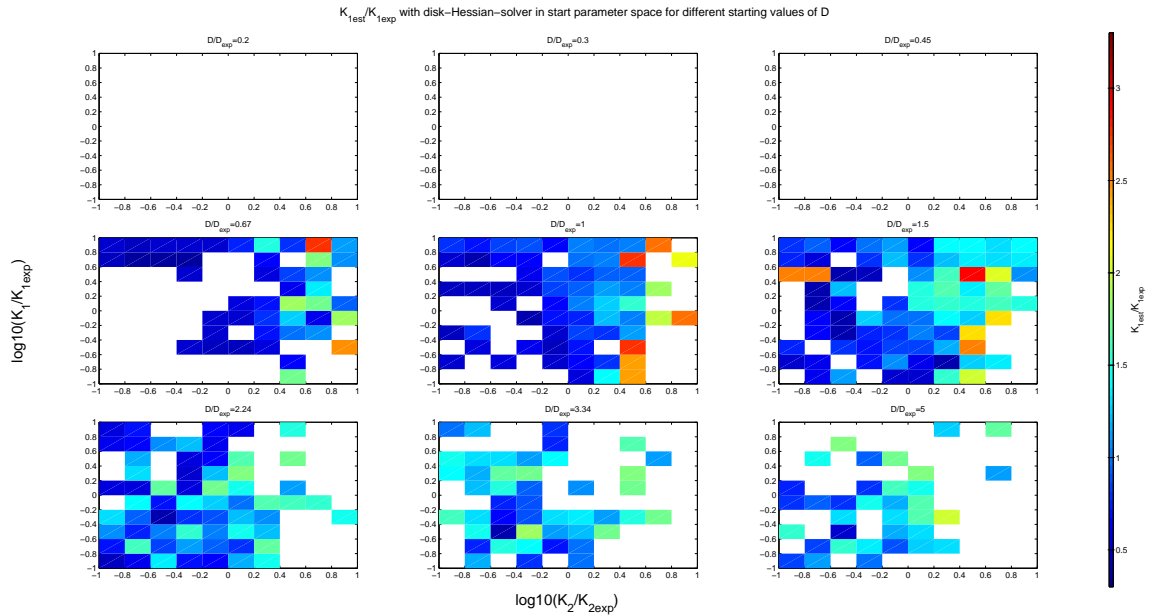


Figure 19: Hessian-solver estimations of K_1 in start parameter space for different D_{start} scale 10

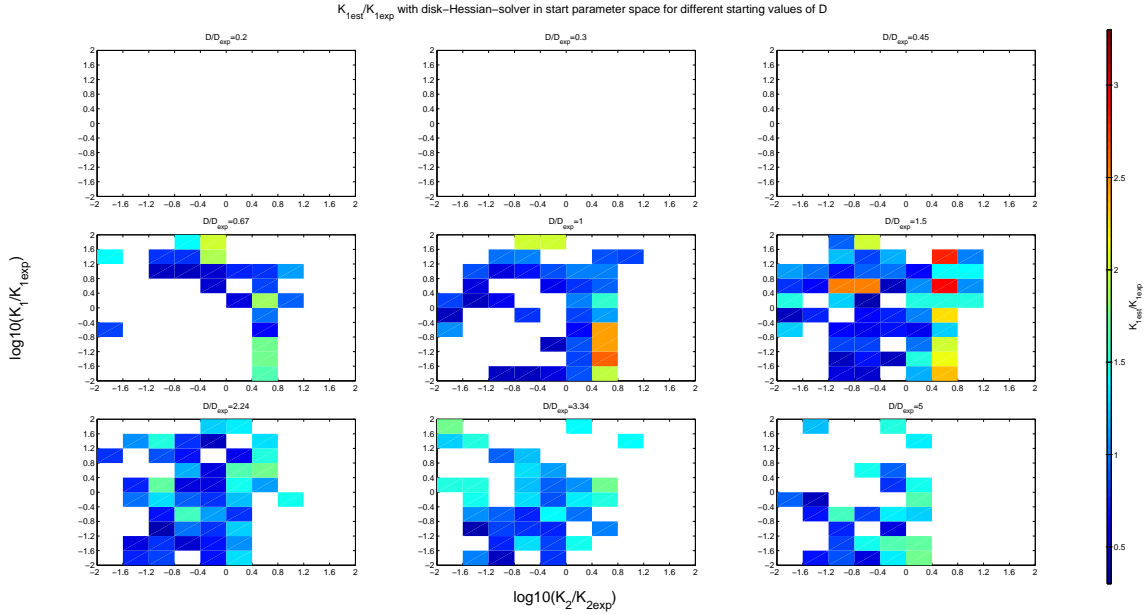


Figure 20: Hessian-solver estimations of K_1 in start parameter space for different D_{start} scale 100

Estimation of K_1, K_2 and D by Ring-Model

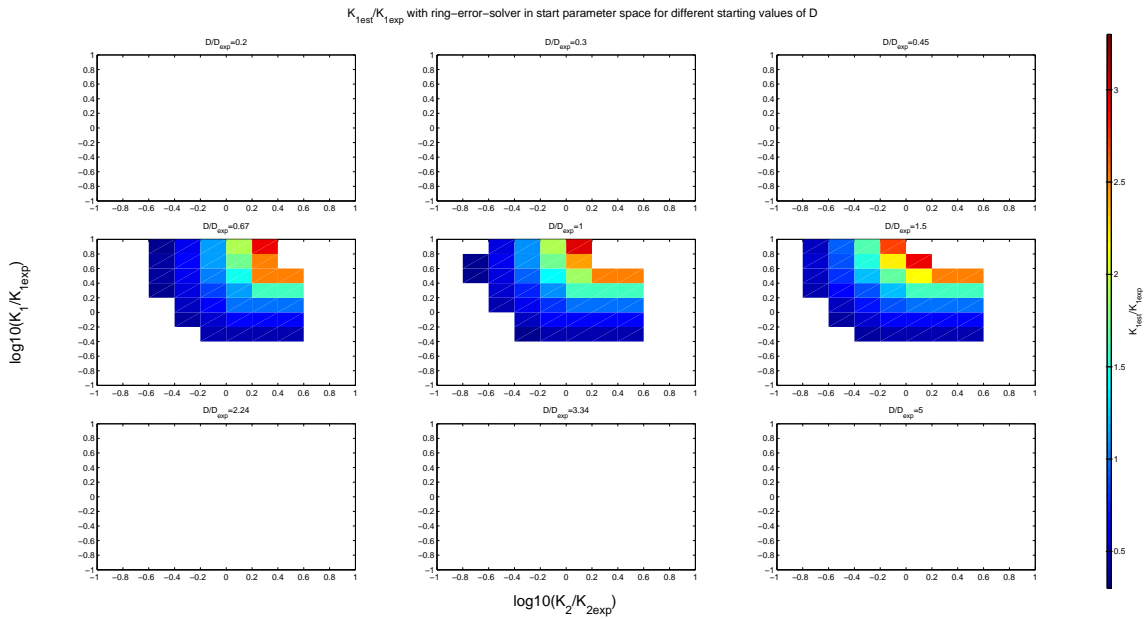


Figure 21: error-solver estimations of K_1 in start parameter space for different D_{start} scale 10

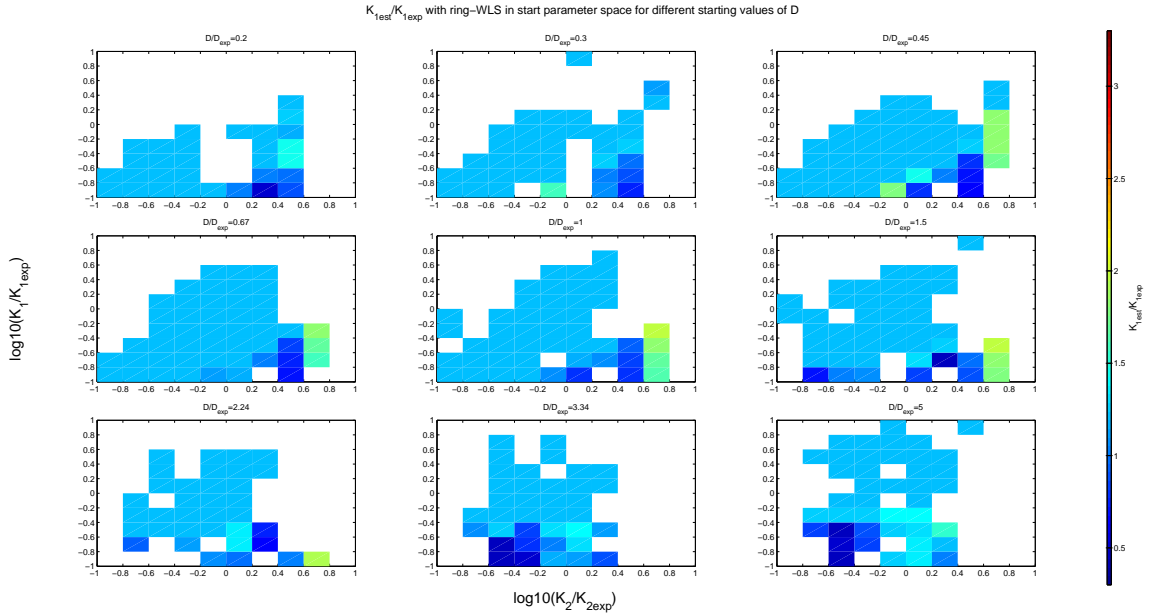


Figure 22: WLS estimations of K_1 in start parameter space for different D_{start} scale 10

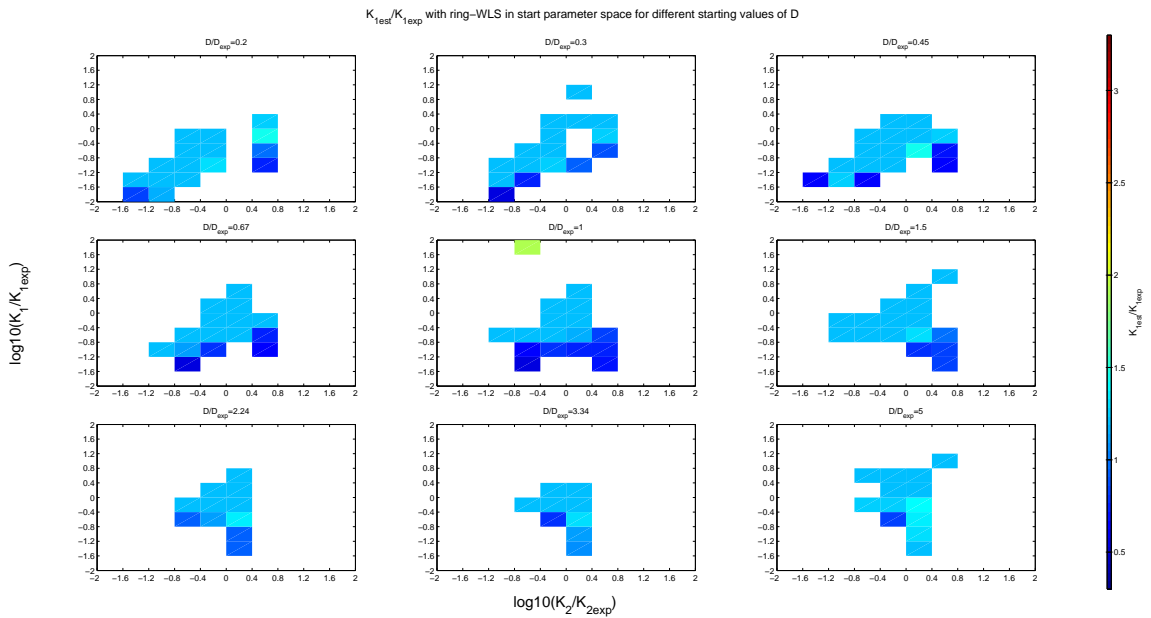


Figure 23: WLS estimations of K_1 in start parameter space for different D_{start} scale 100

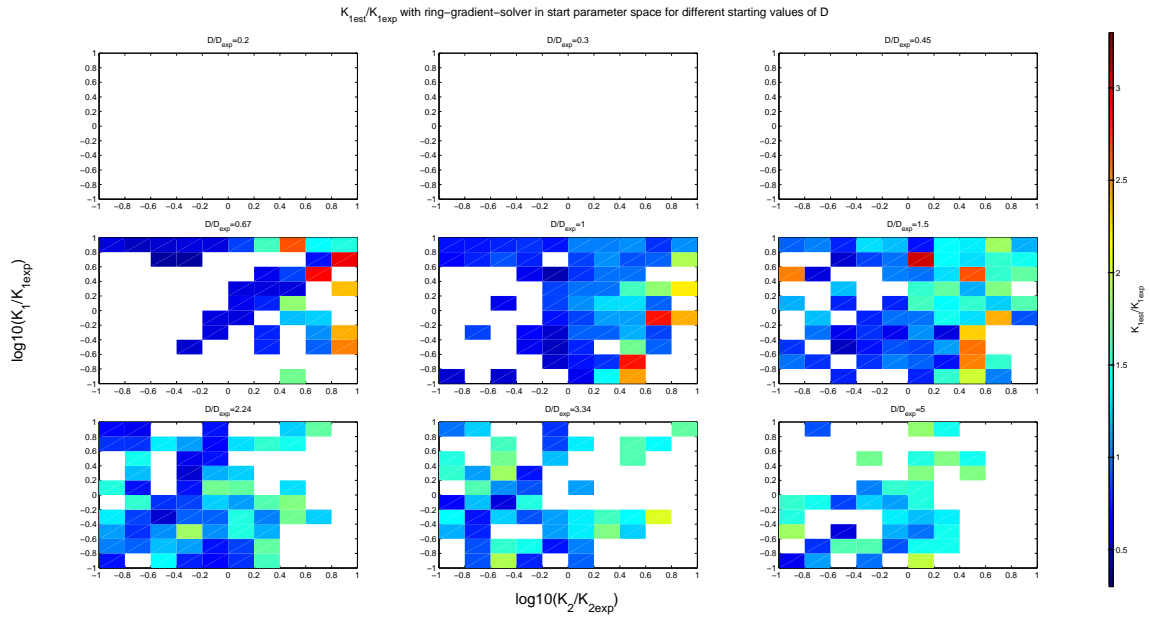


Figure 24: gradient-solver estimations of K_1 in start parameter space for different D_{start} scale 10

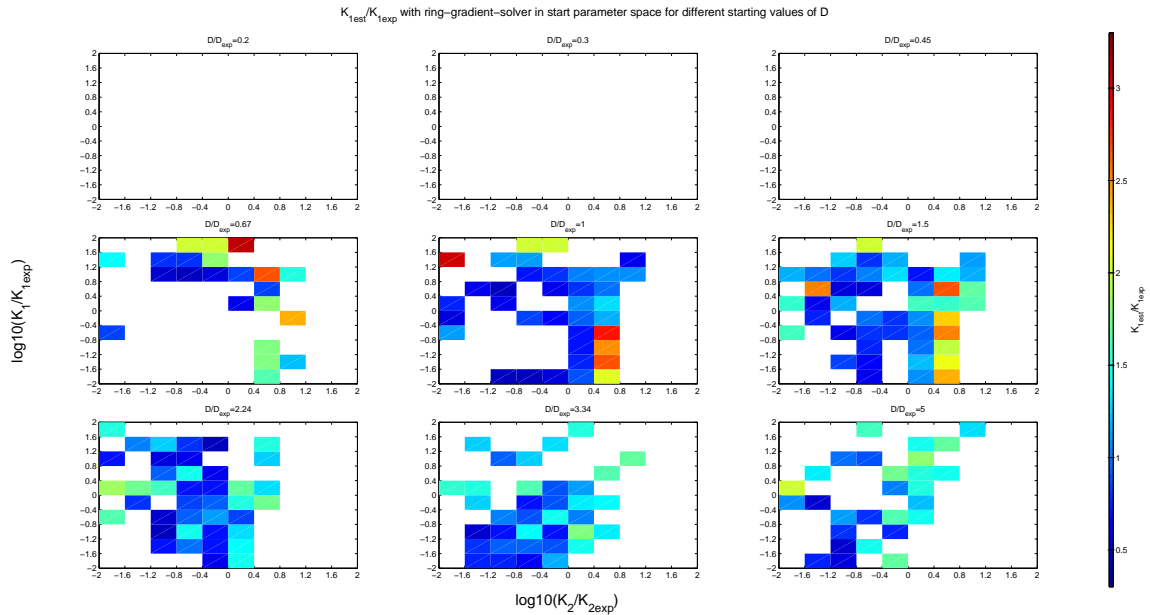


Figure 25: gradient-solver estimations of K_1 in start parameter space for different D_{start} scale 100

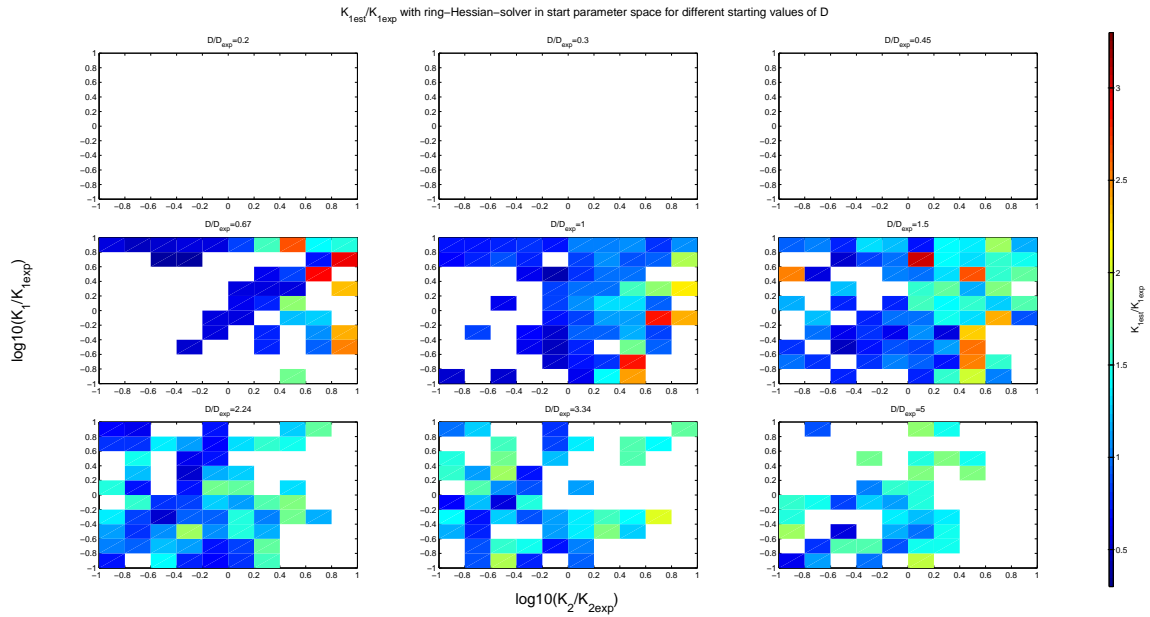


Figure 26: Hessian-solver estimations of K_1 in start parameter space for different D_{start} scale 10

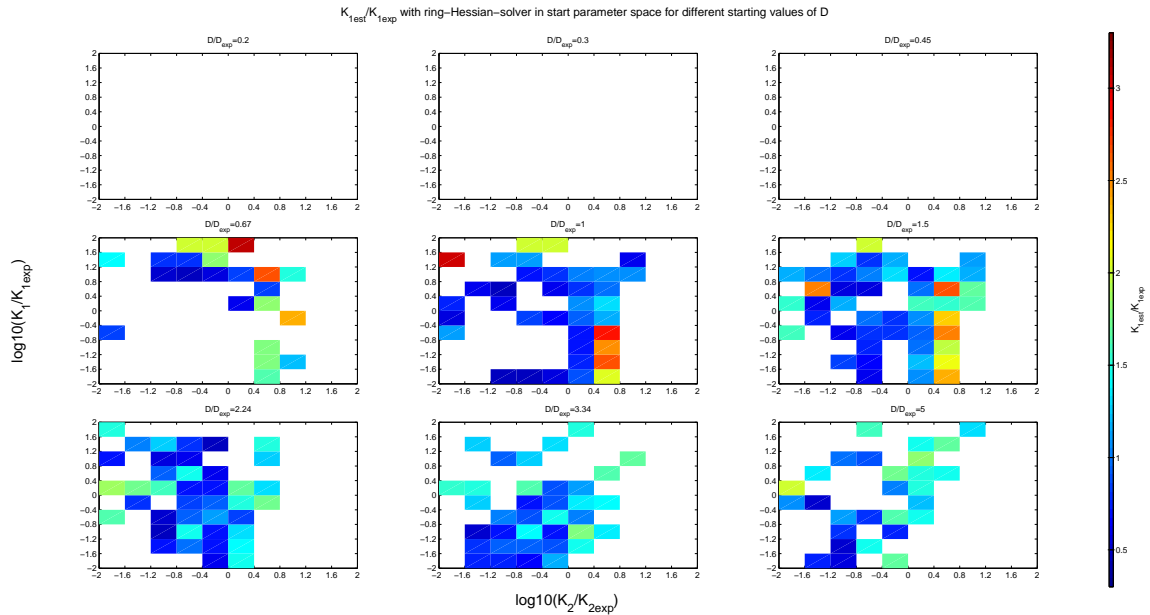


Figure 27: Hessian-solver estimations of K_1 in start parameter space for different D_{start} scale 100

3.3.3 Comparison of Estimators

Terms	Method	t_{est}	it.	K_1	K_2	D
50	WLS	1	8	1.3721	1.5233	1.374e-11
	error-solver	7.52	27	0.9962	1.4696	1.004e-11
	gradient-solver	4.80	13	0.9962	1.4695	1.004e-11
	Hessian-solver	4.32	13	0.9962	1.4695	1.004e-11
	disk-WLS	1.65	6	0.6494	1.3261	0.9493e-11
	disk-error-solver	27.34	31	0.6880	1.3261	0.9493e-11
	disk-gradient-solver	34.35	12	0.6883	1.3263	0.9496e-11
	disk-Hessian-solver	27.00	12	0.6883	1.3263	0.9496e-11
	ring-WLS	21.19	max	0.6909	1.3455	0.9125e-11
	ring-error-solver	28.50	33	0.6908	1.3455	0.9124e-11
	ring-gradient-solver	115.16	41	0.6914	1.3458	0.9128e-11
	ring-Hessian-solver	88.78	41	0.6914	1.3458	0.9128e-11
100	WLS	1.28				
	error-solver	8.75				
	gradient-solver	7.78				
	Hessian-solver	7.32				
	disk-WLS	2.30				
	disk-error-solver	39.74				
	disk-gradient-solver	58.50				
	disk-Hessian-solver	52.86				
	ring-WLS	34.31				
	ring-error-solver	41.34				
	ring-gradient-solver	190.03				
	ring-Hessian-solver	170.52				
500	WLS	3.79				
	error-solver	19.47				
	gradient-solver	37.36				
	Hessian-solver	31.58				
	disk-WLS	8.17				
	disk-error-solver	152.50				
	disk-gradient-solver	304.40				
	disk-Hessian-solver	255.43				
	ring-WLS	150.39				
	ring-error-solver	167.48				
	ring-gradient-solver	962.78				
	ring-Hessian-solver	936.88				

Table 11: Comparison of all implemented estimators for 50, 100 and 500 Terms of the Bessel series

4 Conclusion

The implemented parameter identification methods are designed to work on a wide range of different experiments. It is proofed that the shown FRAP models reproduce real measurements as an accurate representation. The successful estimation of the parameters by the implemented FRAP-models is possible. This is shown on one specific data set and has to be verified by other experiments. The results of the parameter estimation for K_1 , K_2 and D need to be confirmed with experiments. The estimators are compared against robustness against the choice of the start parameters. This comparison can not be generalized. The figures of this comparison plot only one special measurement for one special protein-binding interaction. That's why the comparison of the estimators in the start parameter space leads only to qualitative conclusions. All comparisons were done by the same data set with the same parameters, the corresponding Matlab-scripts can be found on the CD attached to this work.

4.1 Number of Terms for the Bessel Series expansion

A number >50 of Bessel series terms doesn't lead to a higher precision. This is shown for the approximation of the initial distribution (table 2), for two parameter estimation (tables 3, 4, 5), and for three parameter estimation (tables 8,9, 10). The results of the estimations are not sensitive for the variation of the number of Bessel terms >50 (see tables 6 and 11). In respect to the runtime, the number of terms should not exceed 100. The accuracy of the Bessel series expansion is limited through the polynomial approximation of the initial distribution.

4.2 Estimation of K_1 and K_2

The Weighted-Least-Square and Hessian-solver are outstanding in the runtime and in the robustness against the choice of the start parameters. The WLS is the fastest of the implemented estimators (see table 6). In the start parameter space the WLS is superior to the error-solver.(see figure 7,8 and 9). The Hessian-solver is in the ranking of the runtime on second place. For unknown order of magnitude of the parameters, the Hessian-solver is the best choice out of the implemented estimators(see figure 7,8 and 9). This estimator has the same robustness against variation of the start parameters as the gradient-solver, but is superior in the runtime.

4.2.1 Ring and Disk Estimation

The estimation runtime of the FRAP-, disk-FRAP-, and ring-FRAP-estimators are presented in table 6.

Comparison of the Results

The parameter identification for the implemented ring-FRAP-model and disk-FRAP-model, provide moderately different results to the FRAP-model (see table 6). These estimated K_1 s and K_2 s lead to the calculated FRAP curves (figure 28), which are plausible results. Probably well designed experiments can help to restrict the set of solutions.

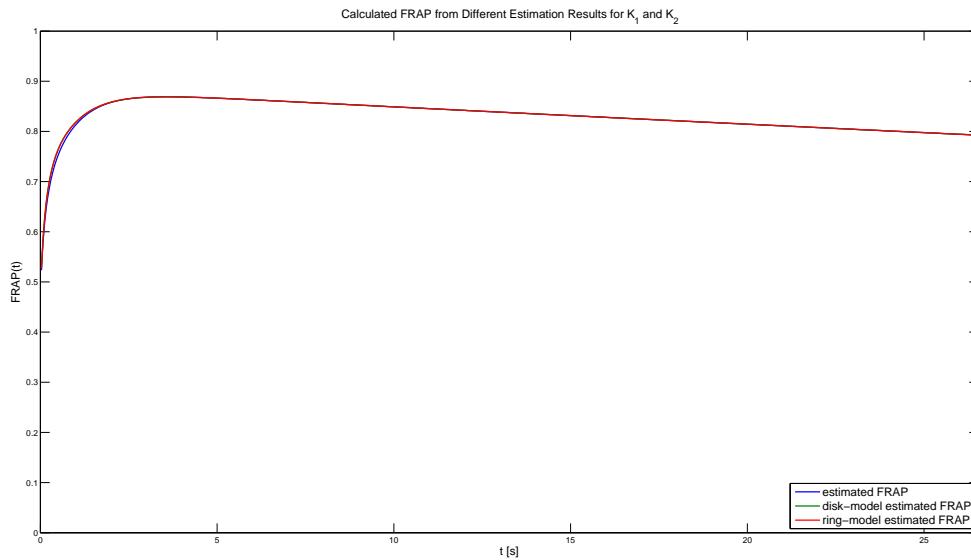


Figure 28: successful estimations of K_1 in start parameter space with different D_{start}

A part of the different results occurs on the assumed variance of the data. The variance is assumed to be equal for these estimations, although the variance is certainly dependent on the averaging area for the FRAP data. The FRAP measurement is averaged over the greatest radius and has the lowest variance of data. The disk FRAP measurement has ascending radii and therefore has descending variances for the different disks. The variance of the ring FRAP data depends on the ring areas (see figure 4, 5 and 6). The estimators are designed to handle variable data variances (time and spatial variant). It is proposed to determine the variances simultaneous with the data acquisition or design an experiment for determining the variances. Those decisions will be left to the user of the estimators.

Covariance Matrix

The reliability of the results has to be investigated, it is represented by the covariance matrix. For the weighted least square estimator the calculation of the covariance is based on an assumed variance of the data. Assuming, that: “The variance is constant over time, and therefore it can be determined through the data before bleaching is processed”. With the pre-bleaching data one can identify the variance for the disk Frap data and of the ring FRAP data. As supposed, the disk FRAP is the most reliable of the implemented estimators. The ring FRAP leads to slightly lower variances than the FRAP-model, although its averaging area is the same size.(see (144),(145) and (146)). Further discussions on the reliability of these results can be done after careful investigation and determination of the variances.

Sensitivity to Choice of Start Parameter

In the start parameter space the spatial estimators have the advantages:

- wider range of possible start parameters
- the results of the estimations become closer

For the given data the disk estimation performs better in the start parameter space than the ring estimation. See figure 7,8 and 9.

4.3 Estimation of K_1 , K_2 and D

The WLS FRAP-model is not suitable for the identification of the three parameters K_1 , K_2 and D (see figure 11), although the other FRAP-model estimators perform better, it is recommended to use the ring or disk estimators (see figures 11-13). The best estimation results can be achieved by the ring or disk WLS (see figures 15, 16, 22 and 23) as it has the highest robustness against variation of D_{start} , precise results for successful estimations and the lowest runtime (see table 11). Whereas the Hessian-solver has a wider range in the $K_{1,start} \times K_{2,start}$ -space for suitable D_{start} s.

Comparison of the Results

The calculated FRAP curves for the different results of the estimators from table 11 are illustrated in figure 29

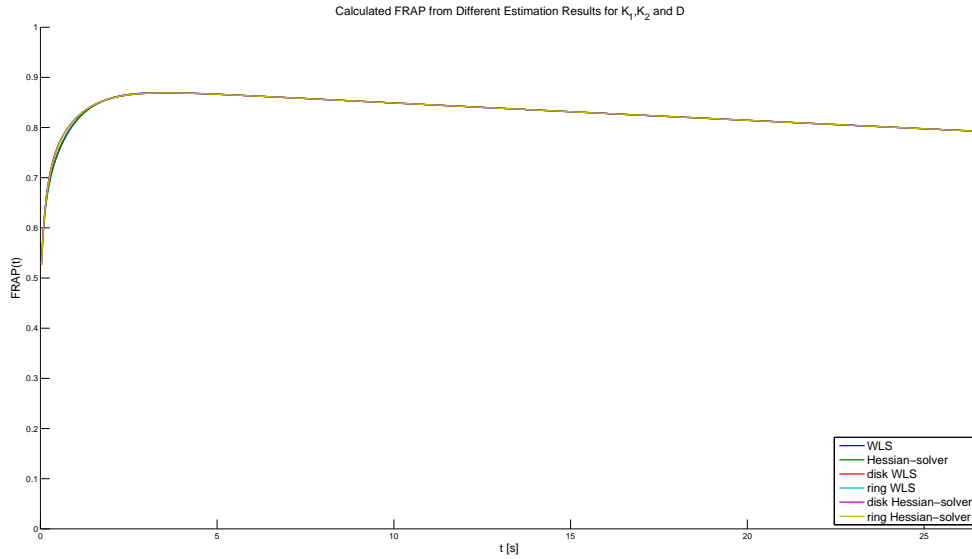


Figure 29: successful estimations of K_1 in start parameter space with different D_{start}

Estimation of D

The estimation of D is possible with the implemented parameter identification, but will lead to a greater uncertainty in the estimation of K_1 and K_2 . It is recommended to determine the diffusion constant in a separate experiment and use the result in the estimation of K_1 and K_2 as this will improve the parameter identification.

References

- [1] D. Axelrod et al. “Mobility measurement by analysis of fluorescence photobleaching recovery kinetics.” In: *Biophys J* 16.9 (1976), pp. 1055–69.
- [2] E.R. Carson, C. Cobelli, and L. Finkelstein. *The mathematical modeling of metabolic and endocrine systems: model formulation, identification, and validation*. Biomedical engineering and health systems. J. Wiley, 1983.
- [3] Per Christian Hansen. *Rank-deficient and discrete ill-posed problems: numerical aspects of linear inversion*. Philadelphia, PA, USA: Society for Industrial and Applied Mathematics, 1998. ISBN: 0-89871-403-6.
- [4] Erwin Kreyszig. *Advanced engineering mathematics*. 6th Revised edition. A76-25,A78-30. Weinheim: Wiley, 1988. ISBN: 0471858242.
- [5] Wilhelm Magnus, Fritz Oberhettinger, and Raj Pal Soni. *Formulas and theorems for the special functions of mathematical physics*. Third Edition. p86-3.8.1, p87-3.10.1, p108-3.8.1, p86-3.8.1. Berlin, Heidelberg, Wien: Springer-Verlag, 1966.
- [6] F. Mueller, P. Wach, and J. G. McNally. “Evidence for a common mode of transcription factor interaction with chromatin as revealed by improved quantitative fluorescence recovery after photobleaching.” In: *Biophys J* 94.8 (2008), pp. 3323–3339. DOI: 10.1529/biophysj.107.123182.
- [7] K. Simonyi. *Theoretischen Elektrotechnik*. p23-No.112],p238-No.107. Berlin: VEB Deutscher Verlag der Wissenschaften, 1980.
- [8] N. Smisdom et al. “Fluorescence recovery after photobleaching on the confocal laser-scanning microscope: generalized model without restriction on the size of the photobleached disk.” In: *J Biomed Opt* 16.4 (2011), p. 046021. DOI: 10.1117/1.3569620.
- [9] B. L. Sprague et al. “Analysis of binding reactions by fluorescence recovery after photobleaching.” In: *Biophys J* 86.6 (2004), pp. 3473–3495. DOI: 10.1529/biophysj.103.026765.

List of Figures

1	raw data in FRAP-curve	3
2	approximating the gaussian decay by linear and quadratic terms	10
3	two approaches for spatial Frap, shown for one timestamp: left Disks, right Rings	28
4	Estimated FRAP and Measured FRAP	33
5	Disks: Estimated FRAP and Measured FRAP	33
6	Rings: Estimated FRAP and Measured FRAP	34
7	estimations in start parameter space	37
8	estimations in start parameter space for disk model	38
9	estimations in start parameter space for ring model	39
10	estimations in start parameter space, error	44
11	estimations in start parameter space, WLS	44
12	estimations in start parameter space, gradient	45
13	estimations in start parameter space, Hessian	45

14	estimations in start parameter space, disks, error	46
15	estimations in start parameter space, disks, WLS	46
16	estimations in start parameter space, disks, WLS	47
17	estimations in start parameter space, disks, gradient	47
18	estimations in start parameter space, disks, gradient	48
19	estimations in start parameter space, disks, Hessian	48
20	estimations in start parameter space, disks, Hessian	49
21	estimations in start parameter space, rings, error	49
22	estimations in start parameter space, rings, WLS	50
23	estimations in start parameter space, rings, WLS	50
24	estimations in start parameter space, rings, gradient	51
25	estimations in start parameter space, rings, gradient	51
26	estimations in start parameter space, rings, Hessian	52
27	estimations in start parameter space, rings, Hessian	52
28	estimations in start parameter space	55
29	estimations in start parameter space	57

List of Tables

2	Effect of Number of Bessel Terms for initial distribution	34
3	Effect of No. of Bessel Terms	35
4	Effect of No. of Bessel Terms in Disk Model	35
5	Effect of No. of Bessel Terms in Ring Model	36
6	Effect of No. of Bessel Terms in Ring Model	40
7	estimated parameters with given variance	41
8	Effect of No. of Bessel Terms	42
9	Effect of No. of Bessel Terms in Disk Model	42
10	Effect of No. of Bessel Terms in Ring Model	43
11	Comparison of Estimators	53

A Appendix

A.1 Determination of Integral over Bessel Functions with Orthogonality Relations

$$\int_0^x x J_n(ax) J_n(bx) dx = \frac{x}{b^2 - a^2} [a J_n(bx) J_n'(ax) - b J_n(ax) J_n'(bx)]$$

$$\int_0^x x J_0(ax) J_0(bx) dx = \frac{x}{b^2 - a^2} [b J_0(ax) J_1(bx) - a J_0(bx) J_1(ax)]$$

[see 7, 238 Nr.107]

$$\alpha_k = \frac{\chi_k}{wR} \quad \alpha_m = \frac{\chi_m}{wR} \quad \chi_k, \chi_m \dots \text{zeros of the Besselfunction of}$$

first kind and first order $J_1(\chi) = 0$

For $\alpha_k \neq \alpha_m$:

$$\begin{aligned} \int_0^{wR} r J_0(\alpha_k r) J_0(\alpha_m r) dr &= \\ &= \frac{r}{\alpha_m^2 - \alpha_k^2} [\alpha_m J_0(\alpha_k wR) J_1(\alpha_m wR) - \alpha_k J_0(\alpha_m wR) J_1(\alpha_k wR)] \\ &= \frac{r}{\alpha_m^2 - \alpha_k^2} [\alpha_m J_0(\chi_k) J_1(\chi_m) - \alpha_k J_0(\chi_m) J_1(\chi_k)] = 0 \end{aligned} \quad (\text{A-1})$$

$$\int_0^x x J_n^2(ax) dx = \frac{x^2}{2} \left[(J_n'(ax))^2 + \left(1 - \frac{n^2}{(ax)^2}\right) J_n^2(ax) \right]$$

[see 7, 23 Nr.112]

For $\alpha_k = \alpha_m$, $\alpha_k \neq 0$:

$$\int_0^{wR} r J_0^2(\alpha_k r) dr = \frac{r^2}{2} \left(\underbrace{J_1^2(\alpha_k wR)}_{\chi_k} + \underbrace{J_0^2(\alpha_k wR)}_{\chi_k} \right) = \frac{r^2}{2} J_0^2(\chi_m) \quad (\text{A-2})$$

For $\alpha_k = 0$:

$$\int_0^{wR} r dr = \frac{r^2}{2} \quad (\text{A-3})$$

$$\int_0^{wR} r J_0(\alpha_k r) J_0(\alpha_m r) dr = \begin{cases} 0 & \alpha_k \neq \alpha_m \\ \frac{r^2}{2} J_0^2(\chi_m) & \alpha_k = \alpha_m \end{cases} \quad (\text{A-4})$$

A.2 Detailed Solution Method for Calculating the Coefficients of the Bessel Series

$$\begin{aligned} & \underline{(-\beta_k + K_2 + K_b)(-\gamma_k + K_2 + K_b)} = \\ & + \beta_k \gamma_k - (K_2 + K_b) \gamma_k - (K_2 + K_b) \beta_k + (K_2 + K_b)^2 = \\ & \beta_k \gamma_k - (K_2 + K_b)(\gamma_k + \beta_k) + (K_2 + K_b)^2 = \\ & w_k^2 - v_k^2 - 2(K_2 + K_b)w_k + (K_2 + K_b)^2 = \\ & [w_k - (K_2 + K_b)]^2 - v_k^2 = \frac{1}{4} (D\alpha_k^2 + K_1 - K_2)^2 - \frac{1}{4} (D\alpha_k^2 + K_1 + K_2)^2 + K_2 D\alpha_k^2 \\ & = \frac{1}{4} \left[\cancel{(D\alpha_k^2 + K_1)} - 2K_2 (D\alpha_k^2 + K_1) + \cancel{K_2^2} - \cancel{(D\alpha_k^2 + K_1)} - 2K_2 (D\alpha_k^2 + K_1) - \cancel{K_2^2} \right] \\ & + K_2 D\alpha_k^2 \\ & = -K_2 (D\alpha_k^2 + K_1) + K_2 D\alpha_k^2 = \underline{\underline{-K_1 K_2}} \end{aligned} \quad (\text{B-1})$$

$$\begin{bmatrix} 1 & 1 \\ K_1 & K_1 \\ -\beta_k + K_2 + K_b & -\gamma_k + K_2 + K_b \end{bmatrix} \begin{bmatrix} A_k \\ B_k \end{bmatrix} = E_k F_{eq} \begin{bmatrix} 1 \\ K_1 \\ K_2 \end{bmatrix} \quad (\text{B-2})$$

$$\frac{1}{\cancel{K_1} K_2} \begin{bmatrix} -\cancel{K_1} K_2 & -\cancel{K_1} K_2 \\ \cancel{K_1} (-\gamma_k + K_2 + K_b) & \cancel{K_1} (-\beta_k + K_2 + K_b) \end{bmatrix} \begin{bmatrix} A_k \\ B_k \end{bmatrix} = F_{eq} \begin{bmatrix} 1 \\ K_1 \\ K_2 \end{bmatrix} E_k \quad (\text{B-3})$$

$$\begin{bmatrix} -K_2 & -K_2 \\ -\gamma_k + K_2 + K_b & -\beta_k + K_2 + K_b \end{bmatrix} \begin{bmatrix} A_k \\ B_k \end{bmatrix} = F_{eq} \begin{bmatrix} -K_2 \\ -K_1 \end{bmatrix} E_k \quad (\text{B-4})$$

$$\begin{aligned}
det &= -K_2(-\beta_k + K_2 + K_b) + K_2(-\gamma_k + K_2 + K_b) \\
&= K_2(-\gamma_k + \beta_k) \\
\begin{bmatrix} A_k \\ B_k \end{bmatrix} &= \frac{1}{det} \begin{bmatrix} -\beta_k + K_2 + K_b & K_2 \\ -(-\gamma_k + K_2 + K_b) & -K_2 \end{bmatrix} \begin{bmatrix} -K_2 \\ -K_1 \end{bmatrix} F_{eq} E_k
\end{aligned}$$

$$\begin{aligned}
A_k &= \frac{1}{\cancel{K_2} \beta_k - \gamma_k} [(-\beta_k + K_2 + K_b) (-\cancel{K_2}) - K_1 \cancel{K_2}] F_{eq} E_k \\
&= \frac{1}{-2v_k} [-\beta_k + K_2 + K_1 + K_b] F_{eq} E_k \quad \checkmark \quad (B-5)
\end{aligned}$$

$$\begin{aligned}
B_k &= \frac{1}{\cancel{K_2} \beta_k - \gamma_k} [(-\gamma_k + K_2 + K_b) \cancel{K_2} + \cancel{K_2} K_1] F_{eq} E_k \\
&= \frac{1}{2v_k} [-\gamma_k + K_2 + K_1 + K_b] F_{eq} E_k \quad \checkmark \quad (B-6)
\end{aligned}$$

$$w_0 = \frac{1}{2} (K_1 + K_2 + 2K_b) \quad (B-7a)$$

$$v_0 = \sqrt{\frac{1}{4} (K_1 + K_2)^2} = \frac{1}{2} (K_1 + K_2) \quad (B-7b)$$

$$\beta_0 = \frac{1}{2} (K_1 + K_2 + 2K_b) + \frac{1}{2} (K_1 + K_2) = K_1 + K_2 + K_b \quad (B-7c)$$

$$\gamma_0 = \frac{1}{2} (K_1 + K_2 + 2K_b) - \frac{1}{2} (K_1 + K_2) = K_b \quad (B-7d)$$

$$-\beta_0 + K_2 + K_b = -K_1 - K_2 - K_b + K_2 + K_b = -K_1$$

$$-\gamma_0 + K_2 + K_b = -K_b + K_2 + K_b = K_2$$

$$A_0 + B_0 = F_{eq} E_0 - F_{eq} = F_{eq} (E_0 - 1)$$

$$A_0 \frac{K_1}{-K_1} + B_0 \frac{K_1}{K_2} = (1 - F_{eq}) E_0 - C_{eq} = (1 - F_{eq}) (E_0 - 1)$$

$$A_0 + B_0 = F_{eq} (E_0 - 1)$$

$$-A_0 + B_0 \frac{K_1}{K_2} = (1 - F_{eq}) (E_0 - 1)$$

$$B_0 \left(1 + \frac{K_1}{K_2}\right) = E_0 - 1$$

$$\underline{B_0 = F_{eq} (E_0 - 1)} \quad \checkmark \quad (B-8)$$

$$\underline{A_0 = 0} \quad \checkmark \quad (B-9)$$

$$\begin{aligned}
a_k &= A_k \frac{K_1}{-\beta_k + K_2 + K_b} \\
a_k &= \frac{1}{-2v_k} \frac{(-\beta_k + K_2 + K_b + K_1) K_1}{-\beta_k + K_2 + K_b} F_{eq} E_k \\
a_k &= -\frac{1}{2v_k} \left[K_1 + \frac{K_1^2}{-\beta_k + K_2 + K_b} \right] F_{eq} E_k \\
a_k &= -\frac{K_1}{2v_k} \left[1 - \frac{\cancel{K_1}(-\gamma_k + K_2 + K_b)}{\cancel{K_1}K_2} \right] F_{eq} E_k \\
a_k &= -\frac{K_1}{K_2} \frac{1}{2v_k} F_{eq} [\cancel{K_2} + \gamma_k - \cancel{K_2} - K_b] E_k \\
a_k &= \frac{1}{2v_k} [-\gamma_k + K_b] (1 - F_{eq}) E_k
\end{aligned} \tag{B-10}$$

$$\begin{aligned}
b_k &= B_k \frac{K_1}{-\gamma_k + K_2 + K_b} \\
b_k &= \frac{1}{2v_k} \frac{(-\gamma_k + K_2 + K_b + K_1) K_1}{-\gamma_k + K_2 + K_b} F_{eq} E_k \\
b_k &= \frac{K_1}{2v_k} \left[1 + \frac{K_1}{-\gamma_k + K_2 + K_b} \right] F_{eq} E_k \\
b_k &= \frac{K_1}{2v_k} \left[1 - \frac{\cancel{K_1}(-\beta_k + K_2 + K_b)}{\cancel{K_1}K_2} \right] F_{eq} E_k \\
b_k &= \frac{1}{2v_k} \frac{K_1}{K_2} [\cancel{K_2} + \beta_k - \cancel{K_2} - K_b] F_{eq} E_k \\
b_k &= -\frac{1}{2v_k} [-\beta_k + K_b] (1 - F_{eq}) E_k
\end{aligned} \tag{B-11}$$

$$\underline{\underline{a_0 = A_0 \frac{K_1}{-\beta_0 + K_2 + K_b} = 0}} \tag{B-12}$$

$$-\gamma_0 + K_2 + K_b = K_2$$

$$-\beta_0 + K_2 + K_b = -(K_1 + \cancel{K_2} + \cancel{K_b}) + \cancel{K_2} + \cancel{K_b} = -K_1 \quad !$$

$$\begin{aligned}
b_0 &= B_0 \frac{K_1}{-\gamma_0 + K_2 + K_b} = F_{eq} (E_0 - 1) \frac{K_1}{K_2} \\
\underline{\underline{b_0 = (1 - F_{eq}) (E_0 - 1)}} & \tag{B-13}
\end{aligned}$$

A.3 Coefficients' Dependence on K_b

v_k ... does not depend on K_b see (15b)

$$A_k = -\frac{1}{2v_k} \left[\underbrace{-w_k + K_b}_{-\overline{w_k}} + K_1 + K_2 \right] F_{eq} E_k \quad (\text{C-1})$$

$\overline{w_k}$... does not depend on K_b see (15a) (C-2)

A_k ... does not depend on K_b (C-3)

the same can be shown for:

$$a_k, B_k, b_k, A_0, a_0, B_0, b_0 \quad (\text{C-4})$$

The coefficients are the same as one would calculate with $K_b = 0$ only

for $\beta_k, \beta_0, \gamma_k, \gamma_0$ K_b is simply added to the solution for $K_b = 0$ (C-5)

For a given K_b we get the solution from the “undamped” solution with $K_b = 0$ by simply multiplying with $e^{-K_b t}$.

A.4 Detailed Partial Derivatives for Frap, Jacobian and rearranged Hessian

$$\begin{aligned} w_k &= 1/2 \left(D\alpha_k^2 + K_1 + K_2 + 2K_b \right) \\ v_k &= \sqrt{1/4 \left(D\alpha_k^2 K_1 K_2 \right)^2 - K_2 D\alpha_k^2} \\ \beta_k &= w_k + v_k \\ Z_k &= (K_b + K_2) D\alpha_k^2 + K_b (K_b + K_1 + K_2) \\ \gamma_k &= \frac{Z_k}{\beta_k} \end{aligned}$$

Partial derivatives of β

$$\frac{\partial \beta_k}{\partial K_1} = \frac{\partial v_k}{\partial K_1} + \frac{\partial w_k}{\partial K_1} \quad (\text{D-1})$$

$$\frac{\partial \beta_k}{\partial K_2} = \frac{\partial v_k}{\partial K_2} + \frac{\partial w_k}{\partial K_2} \quad (\text{D-2})$$

$$\frac{\partial \beta_k}{\partial D} = \frac{\partial v_k}{\partial D} + \frac{\partial w_k}{\partial D} \quad (\text{D-3})$$

$$\frac{\partial^2 \beta_k}{\partial K_1^2} = \frac{\partial^2 v_k}{\partial K_1^2} + \frac{\partial^2 w_k}{\partial K_1^2} \quad (\text{D-4})$$

$$\frac{\partial^2 \beta_k}{\partial K_1 \partial K_2} = \frac{\partial^2 v_k}{\partial K_1 \partial K_2} + \frac{\partial^2 w_k}{\partial K_1 \partial K_2} \quad (\text{D-5})$$

$$\frac{\partial^2 \beta_k}{\partial K_1 \partial D} = \frac{\partial^2 v_k}{\partial K_1 \partial D} + \frac{\partial^2 w_k}{\partial K_1 \partial D} \quad (\text{D-6})$$

$$\frac{\partial^2 \beta_k}{\partial K_2^2} = \frac{\partial^2 v_k}{\partial K_2^2} + \frac{\partial^2 w_k}{\partial K_2^2} \quad (\text{D-7})$$

$$\frac{\partial^2 \beta_k}{\partial K_2 \partial D} = \frac{\partial^2 v_k}{\partial K_2 \partial D} + \frac{\partial^2 w_k}{\partial K_2 \partial D} \quad (\text{D-8})$$

$$\frac{\partial^2 \beta_k}{\partial D^2} = \frac{\partial^2 v_k}{\partial D^2} + \frac{\partial^2 w_k}{\partial D^2} \quad (\text{D-9})$$

Partial derivatives of γ

$$\frac{\partial \gamma_k}{\partial K_1} = \frac{1}{\beta_k^2} \left(\frac{\partial Z_k}{\partial K_1} \beta_k - \frac{\partial \beta_k}{\partial K_1} Z_k \right) \quad (\text{D-10})$$

$$\frac{\partial \gamma_k}{\partial K_2} = \frac{1}{\beta_k^2} \left(\frac{\partial Z_k}{\partial K_2} \beta_k - \frac{\partial \beta_k}{\partial K_2} Z_k \right) \quad (\text{D-11})$$

$$\frac{\partial \gamma_k}{\partial D} = \frac{1}{\beta_k^2} \left(\frac{\partial Z_k}{\partial D} \beta_k - \frac{\partial \beta_k}{\partial D} Z_k \right) \quad (\text{D-12})$$

$$\frac{\partial^2 \gamma_k}{\partial K_1^2} = \frac{1}{\beta_k^3} \left(\beta_k \left(-2 \frac{\partial \beta_k}{\partial K_1} \frac{\partial Z_k}{\partial K_1} - \frac{\partial^2 \beta_k}{\partial K_1^2} Z_k \right) + 2 \frac{\partial \beta_k^2}{\partial K_1} Z_k \right) \quad (\text{D-13})$$

$$\frac{\partial^2 \gamma_k}{\partial K_2^2} = \frac{1}{\beta_k^3} \left(\beta_k \left(-2 \frac{\partial \beta_k}{\partial K_2} \frac{\partial Z_k}{\partial K_2} - \frac{\partial^2 \beta_k}{\partial K_2^2} Z_k \right) + 2 \frac{\partial \beta_k^2}{\partial K_2} Z_k \right) \quad (\text{D-14})$$

$$\frac{\partial^2 \gamma_k}{\partial D^2} = \frac{1}{\beta_k^3} \left(\beta_k \left(-2 \frac{\partial \beta_k}{\partial D} \frac{\partial Z_k}{\partial D} - \frac{\partial^2 \beta_k}{\partial D^2} Z_k \right) + 2 \frac{\partial \beta_k^2}{\partial D} Z_k \right) \quad (\text{D-15})$$

Partial derivatives of $e^{-\beta t}$

$$\frac{\partial e^{-\beta t}}{\partial K_1} = -t \frac{\partial \beta}{\partial K_1} e^{-\beta t} \quad (\text{D-16})$$

$$\frac{\partial e^{-\beta t}}{\partial K_2} = -t \frac{\partial \beta}{\partial K_2} e^{-\beta t} \quad (\text{D-17})$$

$$\frac{\partial e^{-\beta t}}{\partial D} = -t \frac{\partial \beta}{\partial D} e^{-\beta t} \quad (\text{D-18})$$

$$\frac{\partial^2 e^{-\beta t}}{\partial K_1^2} = -t \frac{\partial^2 \beta}{\partial K_1^2} e^{-\beta t} + t^2 \frac{\partial \beta}{\partial K_1}^2 e^{-\beta t} \quad (\text{D-19})$$

$$\frac{\partial^2 e^{-\beta t}}{\partial K_1 \partial K_2} = -t \frac{\partial^2 \beta}{\partial K_1 \partial K_2} e^{-\beta t} + t^2 \frac{\partial \beta}{\partial K_1} \frac{\partial \beta}{\partial K_2} e^{-\beta t} \quad (\text{D-20})$$

$$\frac{\partial^2 e^{-\beta t}}{\partial K_1 \partial D} = -t \frac{\partial^2 \beta}{\partial K_1 \partial D} e^{-\beta t} + t^2 \frac{\partial \beta}{\partial K_1} \frac{\partial \beta}{\partial D} e^{-\beta t} \quad (\text{D-21})$$

$$\frac{\partial^2 e^{-\beta t}}{\partial K_2^2} = -t \frac{\partial^2 \beta}{\partial K_2^2} e^{-\beta t} + t^2 \frac{\partial \beta}{\partial K_2}^2 e^{-\beta t} \quad (\text{D-22})$$

$$\frac{\partial^2 e^{-\beta t}}{\partial K_2 \partial D} = -t \frac{\partial^2 \beta}{\partial K_2 \partial D} e^{-\beta t} + t^2 \frac{\partial \beta}{\partial K_2} \frac{\partial \beta}{\partial D} e^{-\beta t} \quad (\text{D-23})$$

$$\frac{\partial^2 e^{-\beta t}}{\partial D \partial K_2} = -t \frac{\partial^2 \beta}{\partial K_1 \partial K_2} e^{-\beta t} + t^2 \frac{\partial \beta}{\partial K_1} \frac{\partial \beta}{\partial K_2} e^{-\beta t} \quad (\text{D-24})$$

$$\frac{\partial^2 e^{-\beta t}}{\partial D^2} = -t \frac{\partial^2 \beta}{\partial D^2} e^{-\beta t} + t^2 \frac{\partial \beta}{\partial D}^2 e^{-\beta t} \quad (\text{D-25})$$

Partial derivatives of $e^{-\gamma t}$

$$\frac{\partial e^{-\gamma t}}{\partial K_1} = -t \frac{\partial \gamma}{\partial K_1} e^{-\gamma t} \quad (\text{D-26})$$

$$\frac{\partial e^{-\gamma t}}{\partial K_2} = -t \frac{\partial \gamma}{\partial K_2} e^{-\gamma t} \quad (\text{D-27})$$

$$\frac{\partial e^{-\gamma t}}{\partial D} = -t \frac{\partial \gamma}{\partial D} e^{-\gamma t} \quad (\text{D-28})$$

$$\frac{\partial^2 e^{-\gamma t}}{\partial K_1^2} = -t \frac{\partial^2 \gamma}{\partial K_1^2} e^{-\gamma t} + t^2 \left(\frac{\partial \gamma}{\partial K_1} \right)^2 e^{-\gamma t} \quad (\text{D-29})$$

$$\frac{\partial^2 e^{-\gamma t}}{\partial K_1 \partial K_2} = -t \frac{\partial^2 \gamma}{\partial K_1 \partial K_2} e^{-\gamma t} + t^2 \frac{\partial \gamma}{\partial K_1} \frac{\partial \gamma}{\partial K_2} e^{-\gamma t} \quad (\text{D-30})$$

$$\frac{\partial^2 e^{-\gamma t}}{\partial K_1 \partial D} = -t \frac{\partial^2 \gamma}{\partial K_1 \partial D} e^{-\gamma t} + t^2 \frac{\partial \gamma}{\partial K_1} \frac{\partial \gamma}{\partial D} e^{-\gamma t} \quad (\text{D-31})$$

$$\frac{\partial^2 e^{-\gamma t}}{\partial K_2^2} = -t \frac{\partial^2 \gamma}{\partial K_2^2} e^{-\gamma t} + t^2 \left(\frac{\partial \gamma}{\partial K_2} \right)^2 e^{-\gamma t} \quad (\text{D-32})$$

$$\frac{\partial^2 e^{-\gamma t}}{\partial K_2 \partial D} = -t \frac{\partial^2 \gamma}{\partial K_2 \partial D} e^{-\gamma t} + t^2 \frac{\partial \gamma}{\partial K_2} \frac{\partial \gamma}{\partial D} e^{-\gamma t} \quad (\text{D-33})$$

$$\frac{\partial^2 e^{-\gamma t}}{\partial D \partial K_2} = -t \frac{\partial^2 \gamma}{\partial K_1 \partial K_2} e^{-\gamma t} + t^2 \frac{\partial \gamma}{\partial K_1} \frac{\partial \gamma}{\partial K_2} e^{-\gamma t} \quad (\text{D-34})$$

$$\frac{\partial^2 e^{-\gamma t}}{\partial D^2} = -t \frac{\partial^2 \gamma}{\partial D^2} e^{-\gamma t} + t^2 \left(\frac{\partial \gamma}{\partial D} \right)^2 e^{-\gamma t} \quad (\text{D-35})$$

A.5 Differentiation with the Symbolic Toolbox

For the partial derivatives of A_k the symbolic toolbox of Matlab was used. The proceeding is plotted in an short program style example.

```
%Declaration of the symbolic variables (EE for E)
syms K2 K1 D Kb alf2 td EE
%definition of the desired variable
nor=K2/(K1+K2);
ww=1/2*(D*alf2+K1+K2+2*Kb);
vv=sqrt(1/4*(D*alf2+K1+K2)^2-K2*D*alf2);
bet=ww+vv;
gam=ww-vv;
AA=1/2*EE*((bet-K1-K2)*nor-(2*nor-1)*Kb+(nor-1)*gam)/vv
```

The representation of AA depending on $EE, K1, K2, D, alf2$ and Kb is assembled, the output of this AA is set in the command window of Matlab and looks like

```
AA =(EE*((K2/(K1 + K2) - 1)*(K1/2 + K2/2 + Kb + (D*alf2)/2...
```



```

- (1/4*(K1 + K2 + D*alf2)^2 - D*K2*alf2)^(1/2))- Kb*((2*K2)/(K1 + K2) - 1)...
+ (K2*(Kb - K2/2 - K1/2 + (D*alf2)/2)...
+ ((K1 + K2 + D*alf2)^2/4 - D*K2*alf2)^(1/2)))/(K1 + K2))...
/(2*((K1 + K2 + D*alf2)^2/4 - D*K2*alf2)^(1/2))

```

For the sensitivity Matrix we need to differentiate with respect to $K1$

```

%calculate the partial derivative with respect to K1
JA=diff(AA, 'K1')

```

The output of this JA looks like

```

JA = - (EE*((K1/2 + K2/2 + (D*alf2)/2)/(2*((K1 + K2 + D*alf2)^2/4...
- D*K2*alf2)^(1/2)) - 1/2)*(K2/(K1 + K2) - 1)+ (K2*(K1/2 + K2/2 + Kb...
+ (D*alf2)/2 - (1/4*(K1 + K2 + D*alf2)^2 - D*K2*alf2)^(1/2))...
/(K1 + K2)^2 - (K2*((K1/2 + K2/2 + (D*alf2)/2)/(2*((K1 + K2 + D*alf2)^2/4...
- D*K2*alf2)^(1/2)) - 1/2))/(K1 + K2) - (2*K2*Kb)/(K1 + K2)^2...
+ (K2*(Kb - K2/2 - K1/2 + (D*alf2)/2 + ((K1 + K2 + D*alf2)^2/4...
- D*K2*alf2)^(1/2)))/(K1 + K2)^2)/(2*((K1 + K2 + D*alf2)^2/4...
- D*K2*alf2)^(1/2)) - (EE*((K2/(K1 + K2) - 1)*(K1/2 + K2/2...
+ Kb + (D*alf2)/2 - (1/4*(K1 + K2 + D*alf2)^2 - D*K2*alf2)^(1/2))...
- Kb*((2*K2)/(K1 + K2) - 1) + (K2*(Kb - K2/2 - K1/2 + (D*alf2)/2...
+ ((K1 + K2 + D*alf2)^2/4 - D*K2*alf2)^(1/2)))/(K1 + K2))...
*(K1/2 + K2/2 + (D*alf2)/2))/(4*((K1 + K2 + D*alf2)^2/4 - D*K2*alf2)^(3/2))

```

As this notation is long and hard to read, it is rewritten. The symbolic toolbox of Matlab has, with the simple command, a function that can find a simplified representation of a symbolic expression.

```

%search by different algorithms for the nicest representation
JA_s=simple(JA);
%display optimal solution
JA_s

```

```

JA_s = -(D^2*EE*K2*alf2^2*(3*K1 - K2 + D*alf2))...
/(((K1 + K2 + D*alf2)^2 - 4*D*K2*alf2)^(3/2)*(K1 + K2)^2)

```

This representation allows to find a factor, that will simplify the expression in this case vv^3 is chosen.

```

%we predict an factor
JA_vv3=simple(JA*vv^3);

```

```
%display result
JA_vv3
```

This derivative is written as

$$JA_{vv3} = -(D^2 * EE * K2 * alf2^2 * (3 * K1 - K2 + D * alf2)) / (8 * (K1 + K2)^2) / vv^3$$

And with $AA_{K1} = JA_{vv3} / vv^3$ rewritten to equation (95)

```
%display readable
pretty(JA_vv3)
```

The pretty function of Matlab plots fractions in text-mode as an text-image. For the second derivative of AA in respect to K_2 the same procedure is used, the code is written as:

```
%derivative in respect to K2 of Jacobian
HA_vv3=diff(JA_vv3, 'K2');
%simplified for factorization
HA_vv3s=simple(HA_vv3);
%chosen vv^5 of AA
HA_vv5s=simple(HA_vv3*vv^2);
%display result
HA_vv5s
```

The result of this Matlab expressions is:

$$HA_{vv5s} = -(D^2 * EE * alf2^2 * (3 * K1^2 - 5 * K1 * K2 + D * K1 * alf2 - D * K2 * alf2) \dots \\ * (D^2 * alf2^2 + 2 * D * K1 * alf2 - 2 * D * K2 * alf2 + K1^2 + 2 * K1 * K2 + K2^2)) \dots \\ / (32 * (K1 + K2)^3)$$

And with $AA_{K1K2} = HA_{vv5s} / vv^5$ rewritten to equation (99)